DTIC FILE COPY

DNA-TR-87-42

UNDRAINED COMPRESSIBILITY OF SATURATED SOIL

AD-A188 400

S. E. Blouin
J. K. Kwang
Applied Research Associates, Inc.
New England Division
Box 120A
Waterman Road
South Royalton, VT 05068

13 February 1984

Technical Report

CONTRACT No. DNA 001-82-C-0042

Approved for public release;
distribution is unlimited.

THIS WORK WAS SPONSORED BY THE DEFENSE NUCLEAR AGENCY
UNDER RDT&E RMSS CODE B344082466 Y99QAXSA00017 H2590D.

DTIC
ELECTE
NOV 23 1987
E

Prepared for
Director
DEFENSE NUCLEAR AGENCY
Washington, DC 20305-1000

87 11 0 047

UNCLASSIFIED
SECURITY CLASSIFICATION OF THIS PAGE

REPORT DOCUMENTATION PAGE

1a. REPORT SECURITY CLASSIFICATION UNCLASSIFIED	1b. RESTRICTIVE MARKINGS
2a. SECURITY CLASSIFICATION AUTHORITY N/A since Unclassified	3. DISTRIBUTION / AVAILABILITY OF REPORT Approved for public release; distribution is unlimited.
2b. DECLASSIFICATION / DOWNGRADING SCHEDULE N/A since Unclassified	
4. PERFORMING ORGANIZATION REPORT NUMBER(S)	5. MONITORING ORGANIZATION REPORT NUMBER(S) DNA-TR-87-42
6a. NAME OF PERFORMING ORGANIZATION Applied Research Associates, Inc. 6b. OFFICE SYMBOL (If applicable)	7a. NAME OF MONITORING ORGANIZATION Director Defense Nuclear Agency
6c. ADDRESS (City, State, and ZIP Code) New England Division Box 120A, Waterman Road South Royalton, VT 05068	7b. ADDRESS (City, State, and ZIP Code) Washington, DC 20305-1000
8a. NAME OF FUNDING / SPONSORING ORGANIZATION 8b. OFFICE SYMBOL (If applicable) SPSS/Pelkey	9. PROCUREMENT INSTRUMENT IDENTIFICATION NUMBER DNA 001-82-C-0042
8c. ADDRESS (City, State, and ZIP Code)	10. SOURCE OF FUNDING NUMBERS PROGRAM ELEMENT NO. 62715H; PROJECT NO. Y99QAXS; TASK NO. A; WORK UNIT ACCESSION NO. DH005801

11. TITLE (Include Security Classification)
UNDRAINED COMPRESSIBILITY OF SATURATED SOIL

12. PERSONAL AUTHOR(S)
Blouin, Scott E.; Kwang, Jin Kim

13a. TYPE OF REPORT	13b. TIME COVERED	14. DATE OF REPORT (Year, Month, Day)	15. PAGE COUNT
Technical	FROM 811121 TO 840213	840213	72

16. SUPPLEMENTARY NOTATION
This work was sponsored by the Defense NUclear Agency under RDT&E RMSS Code B344082466 Y99QAXSA00017 H2590D.

17. COSATI CODES		
FIELD	GROUP	SUB-GROUP
08	10	
12	01	

18. SUBJECT TERMS (Continue on reverse if necessary and identify by block number)
Liquefaction, Saturated Soils, Soil Mechanics; compressive properties, Mixture Theory;

19. ABSTRACT (Continue on reverse if necessary and identify by block number)
A series of equations for the bulk and constrained compressibility of undrained saturated granular soils are developed. Four sets of equations are developed, each set using a more complicated and realistic set of assumptions describing the soil behavior. A computational parametric analysis describes the applicability of the various assumptions as a function of soil parameters. The parametric analysis can be used to select the simplest suitable soil model applicable to a given problem.

20. DISTRIBUTION / AVAILABILITY OF ABSTRACT ☐ UNCLASSIFIED/UNLIMITED ☒ SAME AS RPT. ☐ DTIC USERS	21 ABSTRACT SECURITY CLASSIFICATION UNCLASSIFIED
22a. NAME OF RESPONSIBLE INDIVIDUAL Sandra E. Young	22b TELEPHONE (Include Area Code) (202)325-7042 22c. OFFICE SYMBOL DNA/CSTI

DD FORM 1473, 84 MAR 83 APR edition may be used until exhausted. All other editions are obsolete.

SECURITY CLASSIFICATION OF THIS PAGE
UNCLASSIFIED

TABLE OF CONTENTS

SECTION		PAGE
	List of Illustrations	iv
1	Introduction.	1
2	Material Models	3
3	Material Model and Parametric Analysis.	26
4	List of References.	59

Accession For
NTIS GRA&I [X]
DTIC TAB [ ]
Unannounced [ ]
Justification
By
Distribution/
Availability Codes
Dist | Avail and/or Special
A-1

LIST OF ILLUSTRATIONS

FIGURE		PAGE
1	Saturated soil/water mixture under hydrostatic compression, schematic section view.	23
2	Schematic section view of the decoupled model under hydrostatic compression.	24
3	Schematic section view of the decoupled model under constrained (uniaxial strain) loading.	25
4	Constrained modulus vs. initial porosity for uncemented sand.	34
5	Constrained modulus vs. initial porosity for coral.	35
6a	Undrained bulk modulus as a function of porosity, uncemented sand.	36
6b	Undrained bulk modulus for uncemented sand, deviation from fully coupled model	37
7a	Undrained bulk modulus as a function of porosity, coral	38
7b	Undrained bulk modulus for coral, deviation from fully coupled model	39
8a	Undrained constrained modulus as a function of porosity, uncemented sand	40
8b	Undrained constrained modulus for uncemented sand, deviation from fully coupled model.	41
9a	Undrained constrained modulus as a function of porosity, coral.	42
9b	Undrained constrained modulus for coral, deviation from fully coupled model	43
10a	Undrained bulk modulus as a function of grain bulk modulus, uncemented sand at 35% porosity	44
10b	Undrained bulk modulus for uncemented sand at 35% porosity, deviation from fully coupled model.	45
11a	Undrained bulk modulus as a function of grain bulk modulus, coral at 35% porosity	46

LIST OF ILLUSTRATIONS (concluded)

FIGURE		PAGE
11b	Undrained bulk modulus for coral at 35% porosity, deviation from fully coupled model.	47
12a	Undrained constrained modulus as a function of grain bulk modulus, uncemented sand at 35% porosity.	48
12b	Undrained constrained modulus for uncemented sand at 35% porosity, deviation from fully coupled model.	49
13a	Undrained constrained modulus as a function of grain bulk modulus, coral at 35% porosity	50
13b	Undrained constrained modulus for coral at 35% porosity, deviation from fully coupled model.	51
14a	Undrained bulk modulus as a function of grain bulk modulus, uncemented sand at 50% porosity	52
14b	Undrained bulk modulus for uncemented sand at 50% porosity, deviation from fully coupled model.	53
15a	Undrained bulk modulus as a function of grain bulk modulus, coral at 50% porosity	54
15b	Undrained bulk modulus for coral at 50% porosity, deviation from fully coupled model.	55
16	Undrained constrained modulus as a function of grain bulk modulus, uncemented sand at 50% porosity	56
17a	Undrained constrained modulus as a function of grain bulk modulus, coral at 50% porosity	57
17b	Undrained constrained modulus for coral at 50% porosity, deviation from fully coupled model.	58

SECTION 1

INTRODUCTION

Analysis of high intensity dynamic loadings of saturated in situ soil deposits requires more sophisticated effective stress models than are used in conventional soil mechanics. The low intensity loadings and slow rates of application of concern in most conventional work permit the use of simplifying assumptions. For instance, the compressibility of the solid grains is usually ignored and even the compressibility of the pore water can often be neglected. Such simplifying assumptions, however, can lead to large errors when used to describe soil response to high intensity, rapidly applied loads such as those from explosive detonations.

Detailed modeling and analysis of the response of saturated soil deposits to explosive loadings require development of finite difference and/or finite element computer codes which delineate the stresses and strains in both the pore water and the soil skeleton. Irreversible volume reductions in the soil skeleton can result in liquefaction and drastically altered behavior of the soil mass. Use of effective stress models which describe the action of the soil skeleton within the pore water are required to properly model and analyze this type of behavior.

While the simplifying assumptions used in conventional soil mechanics are not relevant to the high intensity dynamic loadings, other simplifying assumptions can sometimes be employed without significantly degrading the accuracy of the dynamic models. These might include ignoring volume strain in the soil particles resulting from effective stress and ignoring skeletal strain resulting from compression of the individual soil particles by pressure in the pore water. Use of such assumptions can significantly simplify effective stress models and greatly reduce computational time and cost. Applicability of such assumptions is a function of the in situ soil properties and the loading function, and should be determined on a case by case basis.

The following sections develop a series of equations for the bulk and constrained compressibility of undrained saturated granular soils in terms of

parameters describing the pore water, the soil grains and the soil skeleton. Four sets of equations are developed, each set being dependent on a more complicated and realistic set of assumptions describing the soil behavior. Finally, a series of parameter studies is presented which graphically describes the applicability of the various assumptions as a function of soil parameters. These parametric studies can be used to aid in selection of the simplest soil model applicable to a given problem.

SECTION 2

MATERIAL MODELS

2.1 MIXTURE MODEL.

2.1.1 Bulk Modulus.

The simplest applicable compressibility model for high stress, rapid loadings of fully saturated soils is the mixture model in which only the compressibility of the pore water and the compressibility of the solid grains by the pore fluid pressure are considered. Strictly speaking, this model is only applicable to suspensions, where intergranular (effective) stress is zero. As will be demonstrated in Section 3, however, it is a reasonably accurate representation of compressibility for uncemented low density saturated soils.

The bulk modulus of the soil-water mixture, K_m, is derived from the relationships illustrated in Figure 1. A total pressure P acts on an element of saturated soil made up entirely of solid grains and water. The total volume of the soil element is given by V_t and the total volumes of the pore water and solid grains within the element are given by V_w and V_g, respectively,

Thus,

$$V_t = V_w + V_g \tag{1}$$

and the porosity n is given by

$$n = \frac{V_w}{V_t} \tag{2}$$

Also,

$$1 - n = \frac{V_g}{V_t} \tag{3}$$

The total strain in the soil element, ε_t, is given by

$$\varepsilon_t = \frac{P}{K_m} \tag{4}$$

where K_m is the bulk modulus of the soil-water mixture. The volume change in the soil element, ΔV, equals the sum of the volume change in the pore water ΔV_w and the total volume change in the solid grains ΔV_g, according to

$$\Delta V = \Delta V_w + \Delta V_g \tag{5}$$

The volume change can also be expressed in terms of total volume as

$$\Delta V = \varepsilon_t V_t \tag{6}$$

Assuming that there is no flow of pore water into or out of the soil element during loading, the volume change in the pore water is given by

$$\Delta V_w = \varepsilon_w V_w \tag{7}$$

where ε_w is volume strain in the pore water. In turn, pore water strain can be expressed by

$$\varepsilon_w = \frac{P}{K_w} \tag{8}$$

where K_w is the bulk modulus of the pore water. Substituting expressions for pore water strain from Equation 8 and the volume of water from Equation 2 into 7 gives

$$\Delta V_w = \frac{P}{K_w} n V_t \tag{9}$$

The total volume change in the soil grains is given by

$$\Delta V_g = \varepsilon_g V_g \tag{10}$$

where ε_g is the volume strain in the solid grains. Assuming that the volume strain in the grains results solely from the action of the pore water pressure P on each individual grain, the strain is given by

$$\varepsilon_g = \frac{P}{K_g} \tag{11}$$

where K_g is the bulk modulus of the solid grains. Expressions for strain from Equation 11 and for granular volume from 3 are substituted into Equation 10 giving

$$\Delta V_g = \frac{P}{K_g} (1 - n) V_t \tag{12}$$

It should be noted that the above assumptions ignore any contribution of effective stress in the soil skeleton to the compressibility of the soil element. Thus, only the properties of the soil-water mixture contribute to the overall compressibility.

Substitution of Equations 6, 9 and 12 into Equation 5 gives an expression for total strain of

$$\varepsilon_t = P\left[\frac{K_w + n(K_g - K_w)}{K_g K_w}\right] \tag{13}$$

Further substitution of Equation 13 into 4 gives the bulk modulus of the soil-water mixture as

$$\boxed{K_m = \frac{K_g K_w}{K_w + n(K_g - K_w)}} \tag{14}$$

Equation 14 is a form of the Wood equation discussed by Richart et al., 1970.

2.1.2 Constrained Modulus.

Since the assumptions used to derive the bulk modulus of the mixture ignore any contribution of intergranular stress, the soil element must behave as a dense fluid. Under uniaxial strain loading, the lateral pressure will equal the applied stress, and the constrained modulus must equal the bulk modulus. Thus, the constrained modulus of the mixture, M_m, is given by

$$\boxed{M_m = K_m = \frac{K_g K_w}{K_w + n(K_g - K_w)}} \tag{15}$$

2.2 DECOUPLED MODEL.

2.2.1 Bulk Modulus.

While the compressibility of the soil-water mixture is a satisfactory approximation of material compressibility for some loose uncemented soils, the contribution of the soil skeleton is often of significance. The simplest method of accounting for the influence of skeleton compressibility is to assume that the skeleton acts independently of the soil-water mixture. This model, called the decoupled model, is pictured schematically in Figure 2. The total pressure, P, applied to the soil element is resisted partially by pressure in the pore water, u, and partially by effective stress in the soil skeleton, $\bar{P}$. The total pressure is given by

$$P = u + \bar{P} \tag{16}$$

which is the effective stress relationship. Assuming no flow during loading, the strain in the soil skeleton, ϵ_s, must equal the strain in the soil-water mixture, ϵ_m. Each in turn must equal the total strain; thus,

$$\epsilon_t = \epsilon_m = \epsilon_s \tag{17}$$

The total strain can be expressed as

$$\epsilon_t = \frac{P}{K_d} \tag{18}$$

where K_d is the decoupled bulk modulus of the soil element. The strain in the soil-water mixture is given by

$$\epsilon_m = \frac{u}{K_m} \tag{19}$$

where K_m is the bulk modulus of the soil-water mixture derived in the previous subsection. The strain in the skeleton is given by

$$\epsilon_s = \frac{\bar{P}}{K_s} \tag{20}$$

where K_s is the bulk modulus of the skeleton. Substituting expressions for P, u, and $\bar{P}$ from Equations 18, 19 and 20 into Equation 16 gives

$$\epsilon_t K_d = \epsilon_m K_m + \epsilon_s K_s \tag{21}$$

Because all strains are equal, as shown in Equation 17, Equation 21 reduces to

$$\boxed{K_d = K_m + K_s} \tag{22}$$

Thus, the bulk modulus for the decoupled model is simply the sum of the bulk modulus of the mixture and the bulk modulus of the soil skeleton.

2.2.2 Constrained Modulus.

The constrained modulus M_d' for the decoupled model is obtained in a manner similar to that used for the bulk modulus. Figure 3 schematically depicts the uniaxial loading. The applied total stress, σ_v' is resisted by compression of the soil-water mixture due to the pore water pressure, u, and by compression of the soil skeleton by the effective stress $\bar{\sigma}_v$. Thus, total stress is given by

$$\sigma_v = u + \bar{\sigma}_v \tag{23}$$

Though strain is constrained to the direction of the applied stress, Equation 17 still holds, with

$$\varepsilon_t = \frac{\sigma_v}{M_d} \tag{24}$$

and

$$\varepsilon_t = \varepsilon_s = \frac{\bar{\sigma}_v}{M_s} \tag{25}$$

where M_s is the constrained modulus of the soil skeleton. Since the soil-water mixture behaves as a fluid, the strain in the mixture is given by

Equation 19. Combining Equations 19, 24, and 25 in the same way as was done for the bulk modulus, gives a similar equation for the decoupled constrained modulus,

$$\boxed{M_d = K_m + M_s} \tag{26}$$

Thus, the decoupled constrained modulus is simply the sum of the bulk modulus of the soil-water mixture and the constrained modulus of the soil skeleton.

2.3 PARTIALLY COUPLED MODEL.

2.3.1 Bulk Modulus.

The decoupled model adequately predicts the compressibility of saturated soils over a range of porosities. At higher densities, however, it may prove inadequate. A more realistic model can be derived by realizing that the pore water pressure also acts to compress the soil skeleton. The pore water pressure acting on each soil particle results in a volumetric strain, ϵ_{gu}, of

$$\epsilon_{gu} = \frac{u}{K_g} \tag{27}$$

The strain in the soil skeleton resulting from the summation of all strains in the individual particles, will also be ϵ_{gu}. In other words, the soil skeleton undergoes a uniform volume reduction proportional to ϵ_{gu} caused by the reduction in volume of the individual particles. Thus, if a volume of saturated soil, initially submerged at a shallow depth, is lowered to a deeper depth, the soil skeleton will undergo a volume reduction with no increase in effective stress.

The compatibility equations for the partially coupled total strain are:

$$\epsilon_t = \frac{p}{K_p} \tag{28}$$

where K_p is the effective bulk modulus for the partially coupled model;

$$\varepsilon_t = \varepsilon_m = \frac{u}{K_m} \tag{29}$$

where ε_m is the strain in the soil-water mixture due to compression by the pore water pressure; and

$$\varepsilon_t = \varepsilon_s = \frac{\bar{P}}{K_s} + \frac{u}{K_g} \tag{30}$$

where the total strain in the soil skeleton equals the strain resulting from the intergranular stress plus the strain resulting from skeleton compression due to the pore water pressure given in Equation 27.

Substituting the value of $\bar{P}$ from Equation 16 into Equation 30 and setting it equal to 29 gives the pore pressure as

$$u = \frac{P}{K_s\left(\frac{1}{K_m} - \frac{1}{K_g}\right) + 1} \tag{31}$$

Equating 28 and 29 gives

$$K_p = \frac{PK_m}{u} \tag{32}$$

Substituting Equation 31 into 32 gives

$$\boxed{K_p = K_m + K_s - \frac{K_m K_s}{K_g}} \tag{33}$$

or, the partially coupled bulk modulus equals the decoupled modulus modified by subtracting the last term in Equation 33;

$$K_p = K_d - \frac{K_m K_s}{K_g} \tag{34}$$

2.3.2 Constrained Modulus.

In order to obtain the solution for the partially coupled constrained loading, the influence of the pore pressure on the total strain in the skeleton must first be determined. Because lateral strains are zero by definition in the constrained case, this influence is not intuitively obvious. For convenience, assume that the applied stress is vertical and that the major principal effective stress in the skeleton is $\bar{\sigma}_v$ and the resultant radial stress is $\bar{\sigma}_r$. Application of the vertical effective stress alone would result in vertical and radial strains in the unrestrained skeleton of

$$\varepsilon_v = \frac{\bar{\sigma}_v}{E_s} \tag{35}$$

and

$$\varepsilon_r = -\mu \frac{\bar{\sigma}_v}{E_s} \tag{36}$$

where μ is Poisson's ratio and E_s is Young's modulus of the soil skeleton. Assuming that radial effective stress is uniform, the minor and intermediate principal stresses can both be given by $\bar{\sigma}_r$. Application of only the intermediate and minor principal effective stresses result in a vertical strain o.

$$\varepsilon_v = -2\mu \frac{\bar{\sigma}_r}{E_s} \tag{37}$$

and a radial strain of

$$\varepsilon_r = \frac{\bar{\sigma}_r}{E_s} - \mu \frac{\bar{\sigma}_r}{E_s} \tag{38}$$

Equation 38 takes into account that the intermediate and minor principal stress are orthogonal to one another. Finally, the components of strain resulting from compression of the individual soil particles by the pore water pressure are given by

$$\varepsilon_v = \frac{u}{3K_g} \tag{39}$$

and

$$\varepsilon_r = \frac{u}{3K_g} \tag{40}$$

In Equations 39 and 40, the skeletal strain is assumed uniform (i.e. isotropic soil skeleton) and second order terms are ignored.

Summing Equations 35, 37, and 39 gives the total vertical strain as

$$\varepsilon_v = \frac{1}{E_s}\left(\bar{\sigma}_v - 2\mu\bar{\sigma}_r\right) + \frac{u}{3K_g} \tag{41}$$

Summing Equations 36, 38, and 40 gives the radial strain as

$$\varepsilon_r = 0 = \frac{1}{E_s}\left[\bar{\sigma}_r - \mu(\bar{\sigma}_v + \bar{\sigma}_r)\right] + \frac{u}{3K_g} \tag{42}$$

Solving Equation 42 for the radial effective stress gives

$$\bar{\sigma}_r = \frac{\mu}{1-\mu}\bar{\sigma}_v - \frac{uE_s}{3(1-\mu)K_g} \tag{43}$$

Since radial strains are zero, the total strain equals the vertical strain. Substituting Equation 43 into 41 gives

$$\varepsilon_t = \varepsilon_v = \bar{\sigma}_v \frac{(1 - 2\mu)(1 + \mu)}{E_s(1 - \mu)} + \frac{u}{K_g} \frac{1 + \mu}{3(1 - \mu)} \tag{44}$$

Using the elastic relationships between bulk modulus, constrained modulus and Young's modulus;

$$K = \frac{E}{3(1 - 2\mu)} \tag{45}$$

$$M = \frac{E(1 - \mu)}{(1 - 2\mu)(1 + \mu)} \tag{46}$$

$$\frac{K}{M} = \frac{1 + \mu}{3(1 - \mu)} \tag{47}$$

Equation 44 can be rewritten as

$$\varepsilon_t = \frac{\bar{\sigma}_v}{M_s} + \frac{K_s}{K_g M_s} u \tag{48}$$

Comparing Equation 48 to Equation 25 shows that the total skeleton strain is modified by the last term of Equation 48 as a result of the partial coupling assumptions.

The remaining strain compatibility conditions for the partially coupled constrained loading are given by

$$\varepsilon_t = \frac{\sigma_v}{M_p} \tag{49}$$

Where σ_v is the total applied stress and M_p is the partially coupled constrained modulus, and

$$\varepsilon_t = \frac{u}{K_m} \tag{50}$$

Substituting the value for effective stress

$$\bar{\sigma}_v = \sigma_v - u \tag{51}$$

into Equation 48, and equating 48 to 50 gives the pore pressure as

$$u = \frac{\sigma_v K_m K_g}{K_g M_s + K_m K_g - K_s K_m} \tag{52}$$

Equating 49 and 50 gives the partially coupled constrained modulus as

$$M_p = \frac{\sigma_v K_m}{u} \tag{53}$$

Substitution of Equation 52 into 53 gives

$$\boxed{M_p = K_m + M_s - \frac{K_m K_s}{K_g}} \tag{54}$$

Thus, the partially coupled constrained modulus is simply the decoupled constrained modulus from Equation 26 modified by the same term used to obtain the partially coupled bulk modulus in Equation 34;

$$\boxed{M_p = M_d - \frac{K_m K_s}{K_g}} \tag{55}$$

2.4 FULLY COUPLED MODEL.

2.4.1 Bulk Modulus.

In the case of the partially coupled model, the influence of the pore water pressure on the volume change of the skeleton was incorporated into the modulus equations. In the fully coupled model, the influence of effective stress on volume strain in the soil-water mixture is added to the assumptions included in the partially coupled model. Effective stress in the soil grains results in compression of the individual grains and an additional volume decrease in the soil-water mixture not accounted for in the previous models.

From Equation 6, the volume strain in the soil-water mixture is defined as

$$\varepsilon_t = \frac{\Delta V}{V_t} \tag{56}$$

In this case there are two components contributing to the net volume change;

$$\Delta V = \Delta V_m + \Delta \bar{V}_g \tag{57}$$

where ΔV_m is the volume change in the soil-water mixture due to the pore water pressure given by

$$\Delta V_m = \frac{u}{K_m} V_t \tag{58}$$

and $\Delta \bar{V}_g$ is the volume change in the solid grains resulting from the effective stress $\bar{P}$. This intragranular stress, $\bar{\sigma}_g$, is given by

$$\bar{\sigma}_g = \frac{\bar{P}}{1 - n} \tag{59}$$

where 1 - n represents the ratio of the volume of the solid grains to the total volume from Equation 3. Because the grains take up only a portion of the total volume, the actual stress in the grains is greater than the effective stress, $\bar{P}$. Strain in the grains, $\bar{\varepsilon}_g$, due to the effective stress, is given by

$$\bar{\varepsilon}_g = \frac{\bar{\sigma}_g}{K_g} = \frac{\bar{P}}{(1 - n)K_g} \tag{60}$$

and the volume change equals the strain in the grains multiplied by the volume of the grains from Equation 3,

$$\Delta\bar{V}_g = \frac{\bar{P}}{K_g} V_t \tag{61}$$

Substitution of Equations 58 and 61 into Equation 57 gives the net volume change as,

$$\Delta V = \frac{u}{K_m} V_t + \frac{\bar{P}}{K_g} V_t \tag{62}$$

Further substitution of Equation 62 into 56 gives the strain in the soil-water mixture;

$$\varepsilon_t = \frac{u}{K_m} + \frac{\bar{P}}{K_g} \tag{63}$$

The other strain compatibility equations are;

$$\varepsilon_t = \frac{P}{K_f} \tag{64}$$

where K_f is the bulk modulus for the fully coupled model, and

$$\varepsilon_t = \frac{\bar{P}}{K_s} + \frac{u}{K_g} \tag{65}$$

Equation 65 represents the volume strain in the soil skeleton resulting from the effective stress plus the action of the pore water on the individual grains, and is identical to the compatibility equation used in the partially coupled model.

Setting Equation 63 equal to 65 and solving for $\bar{P}$ gives

$$\bar{P} = \beta_k u \tag{66}$$

where

$$\beta_k = \frac{K_s(K_g - K_m)}{K_m(K_g - K_s)} \tag{67}$$

Substituting Equation 16 into 64, equating 64 and 63, and solving for the bulk modulus, K_f, using Equation 66 gives

$$K_f = \frac{(\beta + 1)K_m K_g}{K_g + \beta K_m} \tag{68}$$

Using the value for β_k from Equation 67 and a bit of manipulation gives the bulk modulus as

$$K_f = K_m + K_s - \frac{K_m K_s}{K_g} + K_m K_s \left[\frac{K_m + K_s - \frac{K_m K_s}{K_g} - K_g}{K_g^2 - K_m K_s} \right] \tag{69}$$

This is simply the bulk modulus of the partially coupled model from Equation 33 modified by the last term in 69. K_f can alternatively be expressed as

$$K_f = K_p + K_m K_s \left[\frac{K_m + K_s - \frac{K_m K_s}{K_g} - K_g}{K_g^2 - K_m K_s} \right] \tag{70}$$

Equations 69 and 70 agree with results derived through different approaches by Gassmann (1951), and Merkle and Dass (1983), and also presented by Hamilton (1971) and Clay and Medwin (1977).

2.4.2 Constrained Modulus.

The difference between the fully and partially coupled constrained moduli is in the strain compatibility equation for the volume strain in the soil-water mixture. Volume strain in the fully coupled case results from volumetric compression of the pore water and soil grains by the pore fluid pressure, u, plus volumetric compression of the solid grains by the principal effective stresses, assumed to be $\bar{\sigma}_v$ and $\bar{\sigma}_r$ as in the partially coupled case.

The overall volume strain is given by

$$\varepsilon_t = \frac{\sigma_v}{M_f} \tag{71}$$

where M_f is the fully coupled constrained modulus. The volume strain in the soil skeleton is identical to that for the partially coupled case given in Equation 48 and repeated here,

$$\varepsilon_t = \frac{\bar{\sigma}_v}{M_s} + \frac{K_s}{K_g M_s} u \tag{72}$$

The volume strain in the soil-water mixture is derived in the same manner as that for the fully coupled bulk modulus except that the mean effective stress in the skeleton, $\bar{\sigma}_m$, is used in place of the effective pressure, $\bar{P}$. Thus, the compatibility Equation corresponding to 63 is

$$\varepsilon_t = \frac{u}{K_m} + \frac{\bar{\sigma}_m}{K_g} \tag{73}$$

where

$$\bar{\sigma}_m = \frac{\bar{\sigma}_v + 2\bar{\sigma}_r}{3} \tag{74}$$

Substitution of Equation 43 into 74 gives the mean effective stress in terms of the vertical effective stress as

$$\bar{\sigma}_m = \bar{\sigma}_v \frac{1 + \mu}{3(1 - \mu)} - \frac{2}{9(1 - \mu)} \frac{E_s}{K_g} u \tag{75}$$

Using Equations 45 and 47, Equation 75 can be expressed as

$$\bar{\sigma}_m = \bar{\sigma}_v \frac{K_s}{M_s} + \frac{K_s}{K_g} \left(\frac{K_s}{M_s} - 1 \right) u \tag{76}$$

Substituting Equation 76 into 73, and equating 73 to 72 gives the effective vertical stress as

$$\bar{\sigma}_v = \beta_m u \tag{77}$$

where

$$\beta_m = \frac{K_g^2 M_s + K_m K_s^2 - M_s K_m K_s - K_g K_m K_s}{K_m K_g (K_g - K_s)} \tag{78}$$

Equations 77 and 51 are combined to give

$$\sigma_v = (\beta_m + 1) u \tag{79}$$

The constrained modulus from Equation 71 can be expressed as

$$M_f = \frac{(\beta_m + 1) K_g M_s}{K_s + \beta_m K_g} \tag{80}$$

using Equation 72 for ϵ_t, 79 for σ_v, and 77 for $\bar{\sigma}_v$. Substitution of Equation 78 into 80 gives

$$M_f = \frac{M_s K_g^2 + K_m K_s^2 + K_m K_g^2 - M_s K_m K_s - 2K_m K_g K_s}{K_g^2 - K_m K_s} \tag{81}$$

Further manipulation gives the constrained modulus in the form

$$\boxed{M_f = K_m + M_s - \frac{K_m K_s}{K_g} + K_m K_s \left[\frac{K_m + K_s - \frac{K_m K_s}{K_g} - K_g}{K_g^2 - K_m K_s} \right]} \tag{82}$$

which is a modification of the partially coupled modulus, M_p' from Equation 54 given by

$$\boxed{M_f = M_p + K_m K_s \left[\frac{K_m + K_s - \frac{K_m K_s}{K_g} - K_g}{K_g^2 - K_m K_s} \right]} \tag{83}$$

The modifier in Equation 83 is exactly the same as the modifier for the bulk modulus in Equation 70. These results agree with those derived by Merkle and Dass (1983) using a somewhat different approach.

2.5 SUMMARY.

Equations for the undrained bulk and constrained modulus of saturated granular soil were developed based on four sets of assumptions governing the

material behavior. These assumptions and the resulting equations are summarized in Table 1. The first and simplest set of assumptions is that the soil behaves as a dense fluid. Applied stress is resisted solely by the compression of the pore water and compression of the individual soil grains by the pore water pressure. The resultant mixture model neglects any contribution to stiffness from the soil skeleton.

The second, or decoupled model, assumes that applied stress is resisted by the stiffness of the soil skeleton acting in parallel with the stiffness of the soil-water mixture from model one. The resultant moduli are simply the sum of the mixture modulus and the bulk or constrained modulus of the soil skeleton, as appropriate.

In the third model, designated the partially coupled model, the assumptions for the decoupled model are modified by including compression of the soil skeleton due to pore water pressure acting on the individual grains. The added strain due to the skeleton compression causes the partially coupled moduli to be somewhat smaller than the corresponding decoupled moduli.

The fourth and most complex model, designated the fully coupled model, incorporates all the assumptions of the partially coupled model and also includes the reduction in volume of the soil-water mixture due to the action of effective stress on the individual particles. This additional reduction in volume strain results in values of fully coupled moduli somewhat lower than those of the partially coupled model.

Table 1. Summary of undrained moduli.

MODEL	ASSUMPTIONS	EQUATIONS
1. Mixture	-Dense fluid with compressible pore water and solid grains -Neglects effective stresses in soil skeleton	$K_m = M_m = \frac{K_g K_w}{K_w + n(K_g - K_w)}$
2. Decoupled	-Mixture model acts in parallel with the soil skeleton	$K_d = K_m + K_s$ $M_d = K_m + M_s$
3. Partially Coupled	-Same as 2, but also includes strain in the skeleton resulting from pore pressure on individual grains	$K_p = K_d - \frac{K_m K_s}{K_g}$ $M_p = M_d - \frac{K_m K_s}{K_g}$
4. Fully Coupled	-Same as 3, but also includes volume change in the soil-water mixture due to effective stress on individual grains	$K_f = K_p + K_m K_s \left[\frac{K_m + K_s - \frac{K_m K_s}{K_g} - K_g}{K_g^2 - K_m K_s} \right]$ $M_f = M_p + K_m K_s \left[\frac{K_m + K_s - \frac{K_m K_s}{K_g} - K_g}{K_g^2 - K_m K_s} \right]$

n porosity

K_g Bulk modulus of solid grains

K_s Bulk modulus of soil skeleton

M_s Constrained modulus of soil skeleton

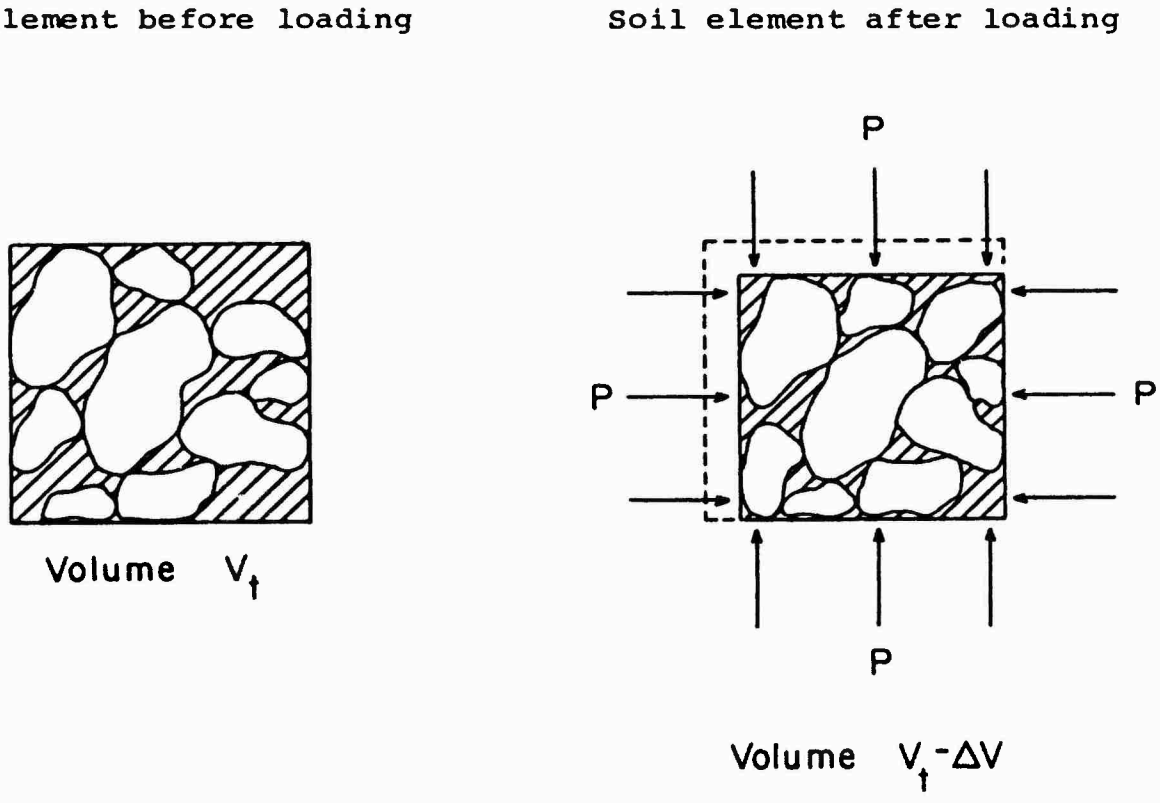

Figure 1. Saturated soil/water mixture under hydrostatic compression, schematic section view.

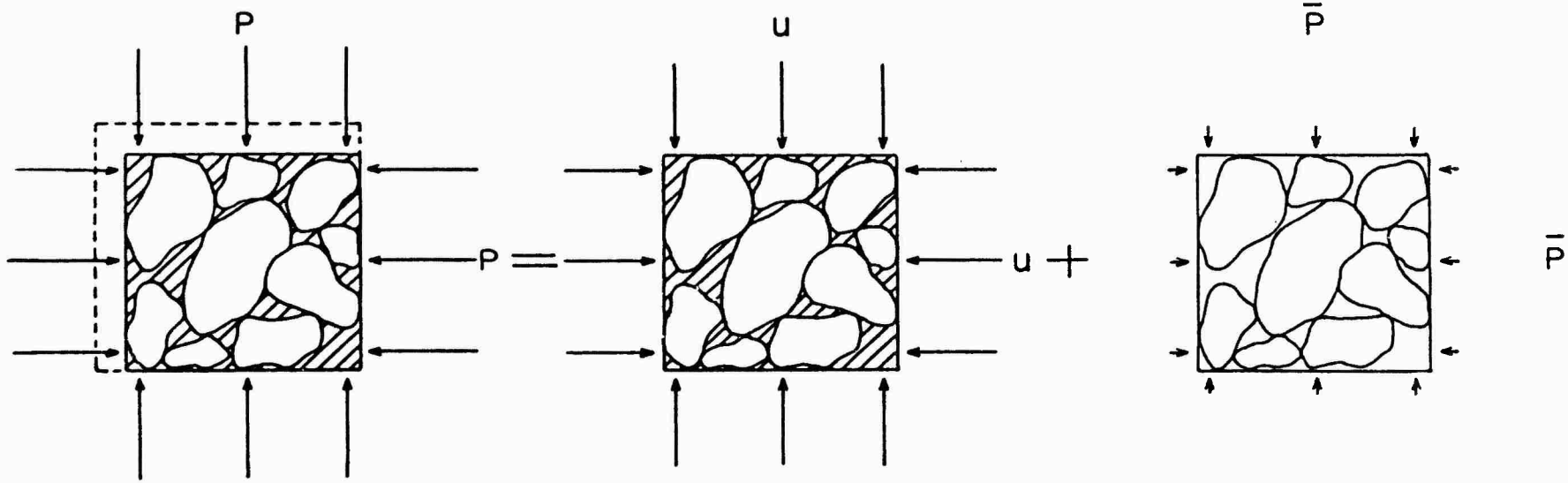

Figure 2. Schematic section view of the decoupled model under hydrostatic compression.

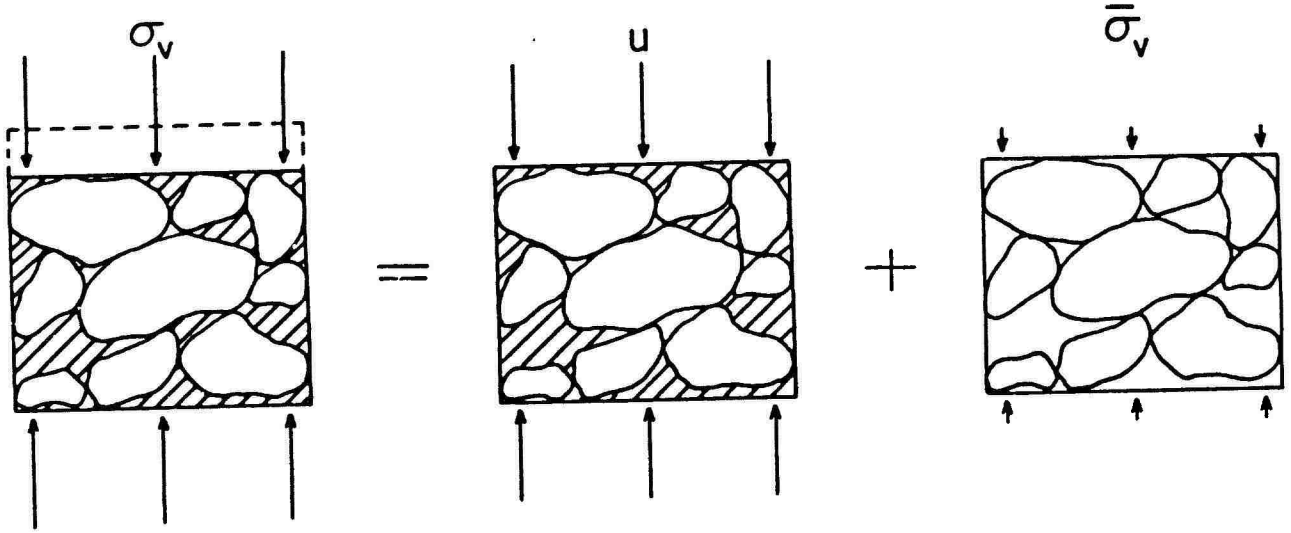

Figure 3. Schematic section view of the decoupled model under constrained (uniaxial strain) loading.

SECTION 3

MATERIAL MODEL AND PARAMETRIC ANALYSIS

3.1 MATERIAL MODEL.

A number of numerical models can be developed based on incremental expressions of the various equations derived in Section 2. Obviously, the complexity of these numerical models will depend on the complexity of the assumptions used in deriving the basic equations. It is desirable to use as simple a model as is adequate for any given problem, thus keeping calculation times and costs to a minimum. In this section, the four models for fully saturated undrained soil, developed in Section 2, are compared as a function of variations in assumed material properties of the soil skeleton. From these comparisons the adequacy of a particular model can be assessed for a particular set of material properties.

In order to study the influence of changes in various soil properties, simplified material models for the soil skeleton were assumed. Models for both uncemented and cemented sands were developed which should bound the behavior of most saturated granular materials. These models express the skeleton bulk and constrained moduli, K_s and M_s as functions of the porosity, n.

Figure 4 shows constrained skeleton moduli from static loadings of 5 different sands as a function of initial porosity. The moduli are the secant moduli measured at a strain of 1.5%. This strain represents the strain at an approximate total stress loading of 1 kbar. A fit to these data was made using the equation

$$M_s = M_g \left(1 - \frac{n}{n_o} \right)^m \tag{84}$$

where M_g is the constrained modulus of the solid grains, n is the porosity, n_o is a limiting porosity, and m is an exponent controlling the shape of the

data fit. At n equal to zero the constrained modulus will equal the modulus of the solid grains.

A constrained modulus of the grains of 9000 ksi was computed using Equation 45, and an assumed bulk modulus, K_g' of 5000 ksi and an assumed Poisson's ratio, μ, of 0.25. The value is representative of typical mineral constituents of many sands. As shown in Figure 4, values of m = 8 and n_o of 0.8 gave a good fit to the uncemented sand data. The data fit is thus expressed as

$$M_s(\text{ksi}) = 9000\left(1 - \frac{n}{0.8}\right)^8 \tag{85}$$

From this equation, an equation for the bulk modulus of the skeleton can be established,

$$K_s(\text{ksi}) = 5000\left(1 - \frac{n}{0.8}\right)^8 \tag{86}$$

Equation 86 assumes that the Poisson's ratio of the skeleton is the same as that of the solid grains (μ = 0.25). In actuality, Poisson's ratio of the skeleton is somewhat greater than Poisson's ratio of the solid grains. Typical values for Poisson's ratio of the skeleton are 0.3, while values for the solid grains range from 0.12 to 0.30. However, in order to simplify the model, Poisson's ratio of the skeleton was assumed equal to that of the grains.

Figure 5 shows values of constrained modulus as a function of porosity for cemented Enewetak coral computed from data given by Pratt and Cooper, 1968. This coral data represents an upper bound for cemented sand, as unconfined compressive strengths ranged from 2.7 to 5.7 ksi. Using an assumed K_g of 5000 ksi, and a representative Poisson's ratio for this material of 0.2, a fit to these data (shown in Figure 5) is given by

$$M_s(\text{ksi}) = 10000 \left(1 - \frac{n}{0.8}\right)^3 \tag{87}$$

The corresponding equation for the bulk modulus of the skeleton is given by

$$K_s(\text{ksi}) = 5000 \left(1 - \frac{n}{0.8}\right)^3 \tag{88}$$

For purposes of this parameter study, Equations 85 through 88 express the moduli solely as functions of porosity. While this is a simplifying assumption, these equations represent reasonable upper and lower bounds to the behavior of actual materials.

3.2 INFLUENCE OF MATERIAL PARAMETERS.

3.2.1 Modulus As A Function of Porosity.

Using the equations for skeleton moduli derived in the previous subsection, the undrained bulk and constrained moduli for the four models summarized in Table 1 are computed as functions of porosity. These results for bulk modulus are shown for the uncemented and cemented cases in Figures 6a and b and 7a and b, respectively. Corresponding plots for the constrained modulus are given in Figures 8a and b and 9a and b. A bulk modulus of water of 300 ksi was assumed in all calculations.

Variation in undrained bulk modulus in the uncemented sand is plotted as a function of porosity for the four models in Figure 6a. For porosities greater than 30%, differences between the four models are insignificant. At the higher porosities, the influence of the soil skeleton is very small, with the overall behavior primarily governed by the soil-water mixture. At the lower porosities, significant differences develop. The lower bound is represented by the mixture model which ignores the stiffness of the soil skeleton. The upper bound is represented by the decoupled model. In the decoupled model the skeleton modulus from Equation 86 is simply superimposed on the mixture modulus. The influence of pore pressure on the skeleton behavior is ignored.

Due to this simple summation, at the limit n = 0, the decoupled modulus approaches $2K_g$. In actuality, the modulus should approach the solid grain modulus, K_g. Thus, the decoupled model introduces large errors at low porosities.

In the decoupled model, the pore pressure acts to reduce the volume of the individual grains and in turn reduces the overall volume of the soil skeleton. This influence of the pore pressure reduces the modulus from that of the decoupled model. At the zero porosity limit, the partially coupled model satisfies compatibility with the solid grain modulus. In the fully coupled model, the modulus is further reduced by additional volume reduction due to the effective stress acting on the solid grains.

Figure 6b compares the mixture, decoupled, and partially coupled models to the fully coupled model. Percent deviation of each of the three models from the fully coupled bulk modulus is shown as a function of porosity. Above a porosity of 28%, deviation in bulk modulus for all the models is less than 10%. This porosity range is representative of nearly all uncemented sands. The decoupled model appears to be entirely adequate in this range of porosities. At 30% porosity, the decoupled bulk modulus is within 4% of the fully coupled modulus.

Bulk modulus as a function of porosity for the cemented material is shown in Figure 7a. Because the skeleton in the cemented case is much stiffer than that in the uncemented case, there is a significant influence of skeleton stiffness over the entire range of porosities. The general trends are the same as those observed in the uncemented material; i.e. the mixture model gives a lower bound modulus, the decoupled model an upper bound modulus, and the partially coupled model a slightly higher modulus than the fully coupled modulus. At the limiting zero porosity, all models except the decoupled are compatible with the solid grain modulus.

Deviation of the mixture, decoupled, and partially coupled moduli from the fully coupled modulus in the cemented material is shown in Figure 7b. As noted above, the mixture modulus deviates significantly from the

fully coupled modulus over the entire range of porosities. At a porosity of 45%, the decoupled modulus is 10% greater than the fully coupled modulus, with deviation increasing rapidly at lower values of n. The partially coupled modulus gives a good approximation of the fully coupled modulus with deviations of less than 10% over the entire range of porosities.

The undrained constrained modulus for the four models in the uncemented material is shown as a function of porosity in Figure 8a. As was the case with the uncemented bulk modulus, there is good agreement between the four models at higher porosities. The mixture and decoupled moduli represent the lower and upper bounds at lower porosities. At zero porosity, however, the mixture modulus no longer converges to the same value as the fully and partially coupled moduli. As shown in the equations of Table 1, the mixture modulus converges to the bulk modulus of the solid grains while the other two moduli converge to the constrained modulus of the solid grains. The decoupled modulus converges to the summation of the bulk and constrained moduli of the solid grains.

The deviation from the fully coupled constrained modulus in the uncemented soil is shown in Figure 8b. The mixture modulus exceeds the fully coupled modulus by more than 10% at porosities of 34% and less. As was the case with the bulk modulus, the decoupled model gives good agreement with the fully coupled model over porosities normally exhibited by uncemented sands. At 30% porosity, the decoupled modulus is only about 3.5% higher than the fully coupled modulus.

In Figure 9a, the constrained moduli in the cemented material are compared over a range of porosities. Due to the high stiffness of the cemented skeleton, the mixture model significantly underestimates the overall modulus at all porosities. Convergence at zero porosity is similar to that in the uncemented material, with the mixture modulus converging to K_g, the partially and fully coupled moduli converging to M_g' and the decoupled modulus converging to $K_g + M_g$. The deviation from the fully coupled model is shown in Figure 9b. Clearly, the mixture model is a poor representation. Deviation of the decoupled model exceeds 10% below porosities of 34%. The partially

coupled model, however, is in good agreement with the fully coupled model over the entire range of porosities, with a maximum deviation from the fully coupled model of less than 5.5%.

From the comparisons in Figures 6a and b through 9a and b it appears that the mixture model is an adequate modulus approximation for many uncemented saturated sands. The decoupled model represents a good modulus approximation for all fully saturated uncemented sands. Suitability of the decoupled model for cemented sands will depend on the in situ porosities and the degree of cementation. For the strongly cemented material presented in this study, the partially coupled model would be a significantly better choice than the decoupled model.

3.2.2 Modulus As A Function of Grain Properties.

Examination of mineral properties reveals a wide variation in moduli. The bulk moduli of materials making up common rocks and sands vary from about 4000 to 15000 ksi, or from about 13 to 50 times the bulk modulus of water. In this subsection, the influence of variation in bulk modulus of the solid grains on the undrained bulk and constrained moduli for the four models is examined. Again, both uncemented and cemented materials are represented, using the skeleton models developed in the first subsection. Two porosities are studied, n = 35%, representative of a dense sand, and n = 50%, representative of a loose sand.

Figure 10a shows bulk modulus as a function of normalized solid grain bulk modulus for the four models at a porosity of 35%. The solid grain modulus is normalized by dividing by the bulk modulus of water (300 ksi). Thus, while normalized modulus varied from 1 to 50, the range from about 13 to 50 represents the range of moduli experienced in common materials. With the exception of the mixture model, the models are in good agreement over the entire range of normalized modulus. The stiffer the grain modulus, the more inadequate is the mixture model. As was the case for modulus variation as a function of porosity, the mixture model represents the lower modulus bound, the decoupled model the upper bound, with the fully coupled model falling just below the partially coupled model.

Percent deviation of the mixture, decoupled and partially coupled models from the fully coupled model for bulk modulus in uncemented soil is shown in Figure 10b. For normalized grain bulk moduli above 35 (10500 ksi), the mixture modulus is more than 10% lower than the fully coupled modulus.

The corresponding bulk modulus plots for cemented sand at 35% porosity are shown in Figures 11a and 11b. Because of the greater stiffness of the skeleton, the modulus variation at low values of normalized bulk modulus is less pronounced than in the cemented soil. For the same reason, the mixture model is much softer than the other models which take skeleton stiffness into account. There is somewhat more difference between the coupled models than was the case in the uncemented material. As shown in Figure 11b, only the partially coupled model is consistently close to the fully coupled model. Deviation is 8% or less over the entire range of normalized bulk modulus.

The constrained modulus and deviation plots for the uncemented sand at 35% porosity are shown in Figures 12a and b. The trends are the same as those of the bulk modulus plots of Figures 10a and b, with close agreement between all the coupled models over the full range of normalized grain modulus. Figures 13a and b are plots of constrained modulus and modulus deviation for the cemented material at 35% porosity. The trends are similar to those for bulk modulus in the cemented material. The decoupled modulus shows less variation from the fully coupled modulus, and the partially coupled modulus is within 6% of the fully coupled modulus over the entire range of grain moduli.

Plots of modulus variation in the uncemented and cemented materials at an initial porosity of 50% are shown in Figures 14a and b through 17a and b. Because the soil skeleton has very little influence on the composite behavior of the uncemented soil, all four of the models for both the bulk and constrained modulus, shown in Figures 14a and b and 16a and b are in very close agreement. The moduli for the cemented material, shown in Figures 15a and b and 17a and b, show the same trends as those at 35% porosity, but with closer overall agreement Both the decoupled and partially coupled moduli are within 8% of the fully coupled modulus over the full range of variation in grain modulus.

In summary, the conclusions drawn from the parametric analysis as a function of porosity hold independent of variations in the modulus of the solid grains. That is, the decoupled model is a satisfactory model for uncemented sands, over all variations in grain modulus. The partially coupled model is a satisfactory model for the cemented material over all variations of grain modulus; though in some instances, the simple decoupled model is also satisfactory.

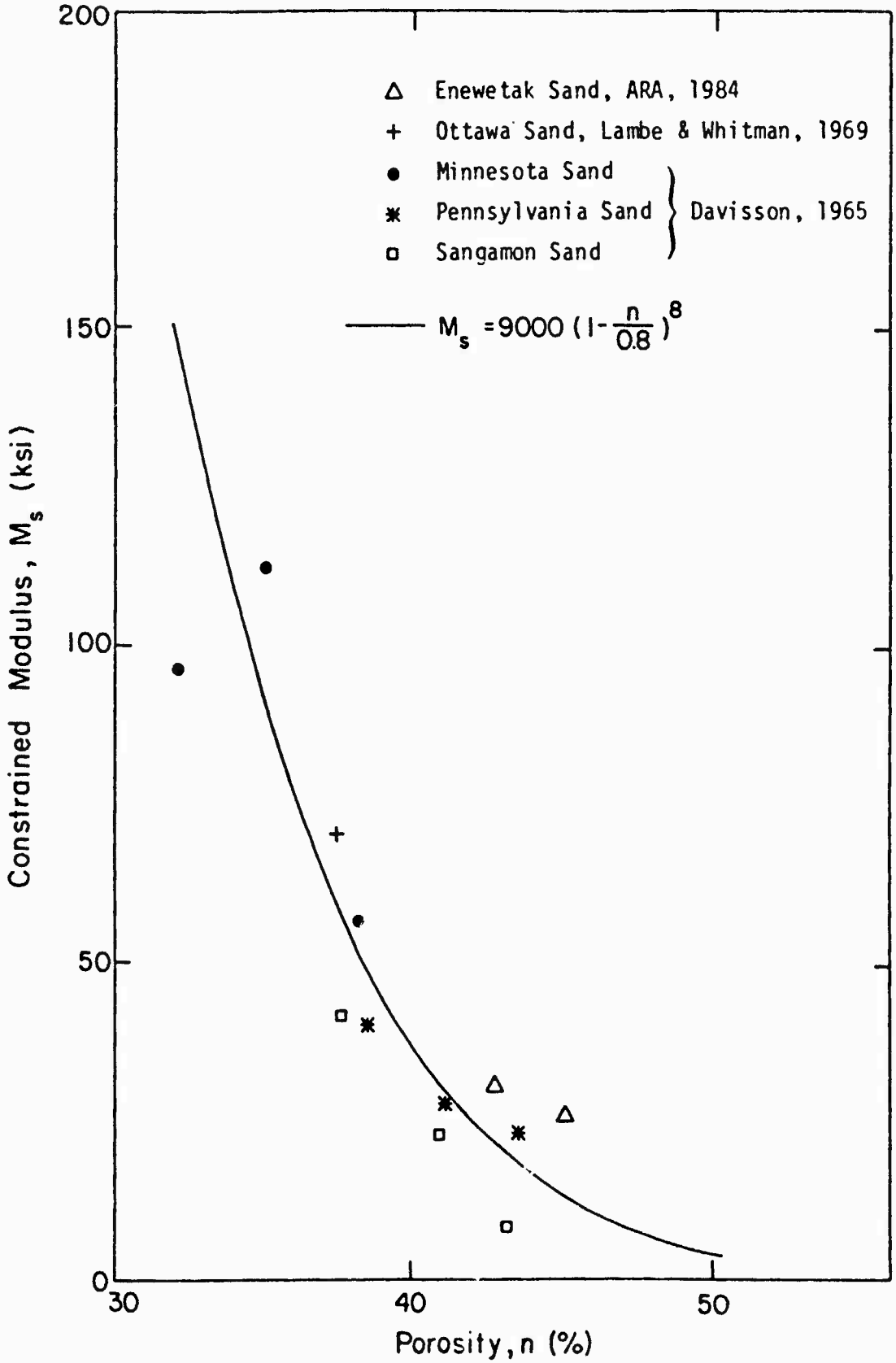

Figure 4. Constrained modulus vs. initial porosity for uncemented sand.

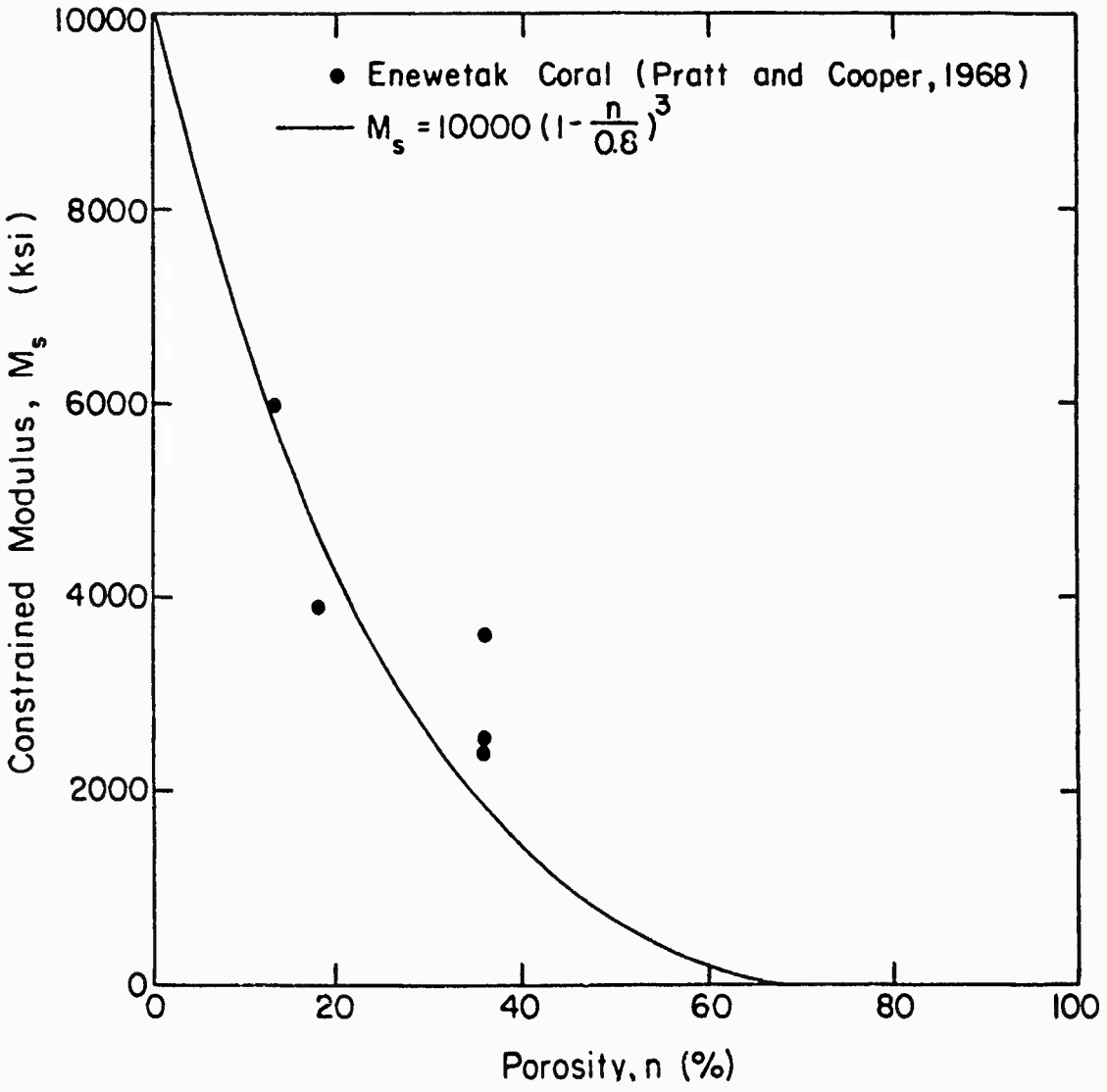

Figure 5. Constrained modulus vs. initial porosity for coral.

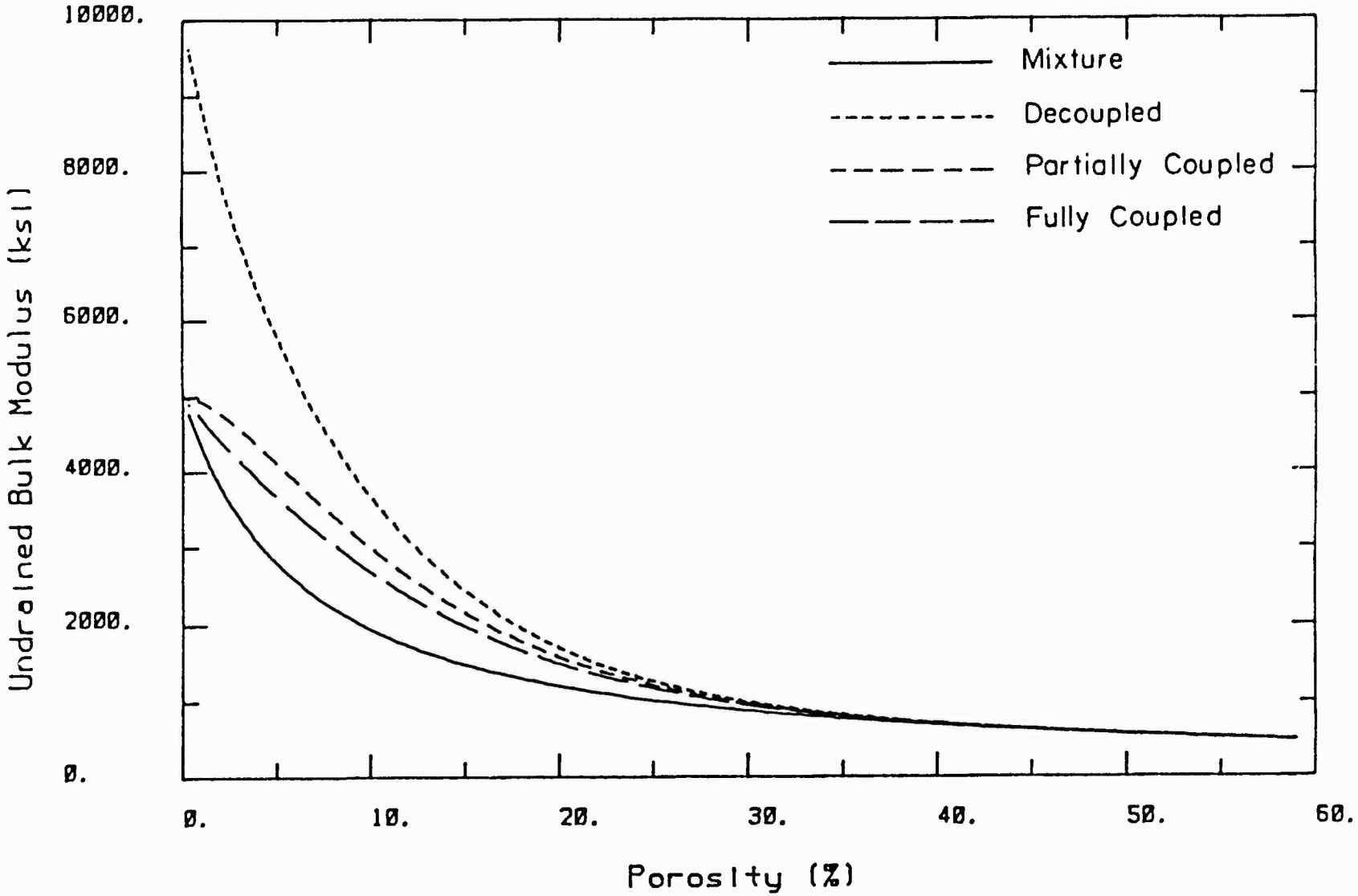

Figure 6a. Undrained bulk modulus as a function of porosity, uncemented sand.

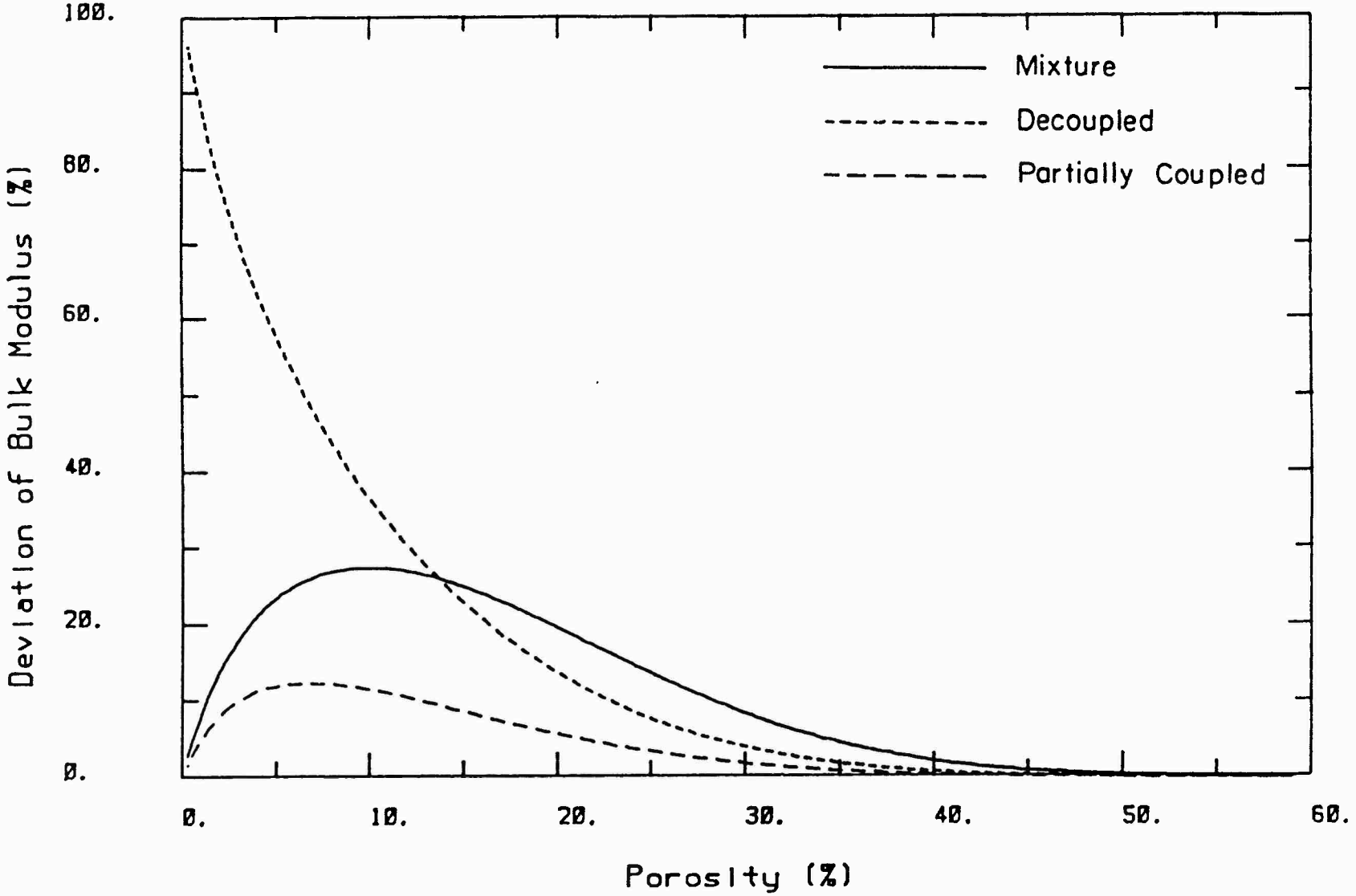

Figure 6b. Undrained bulk modulus for uncemented sand, deviation from fully coupled model.

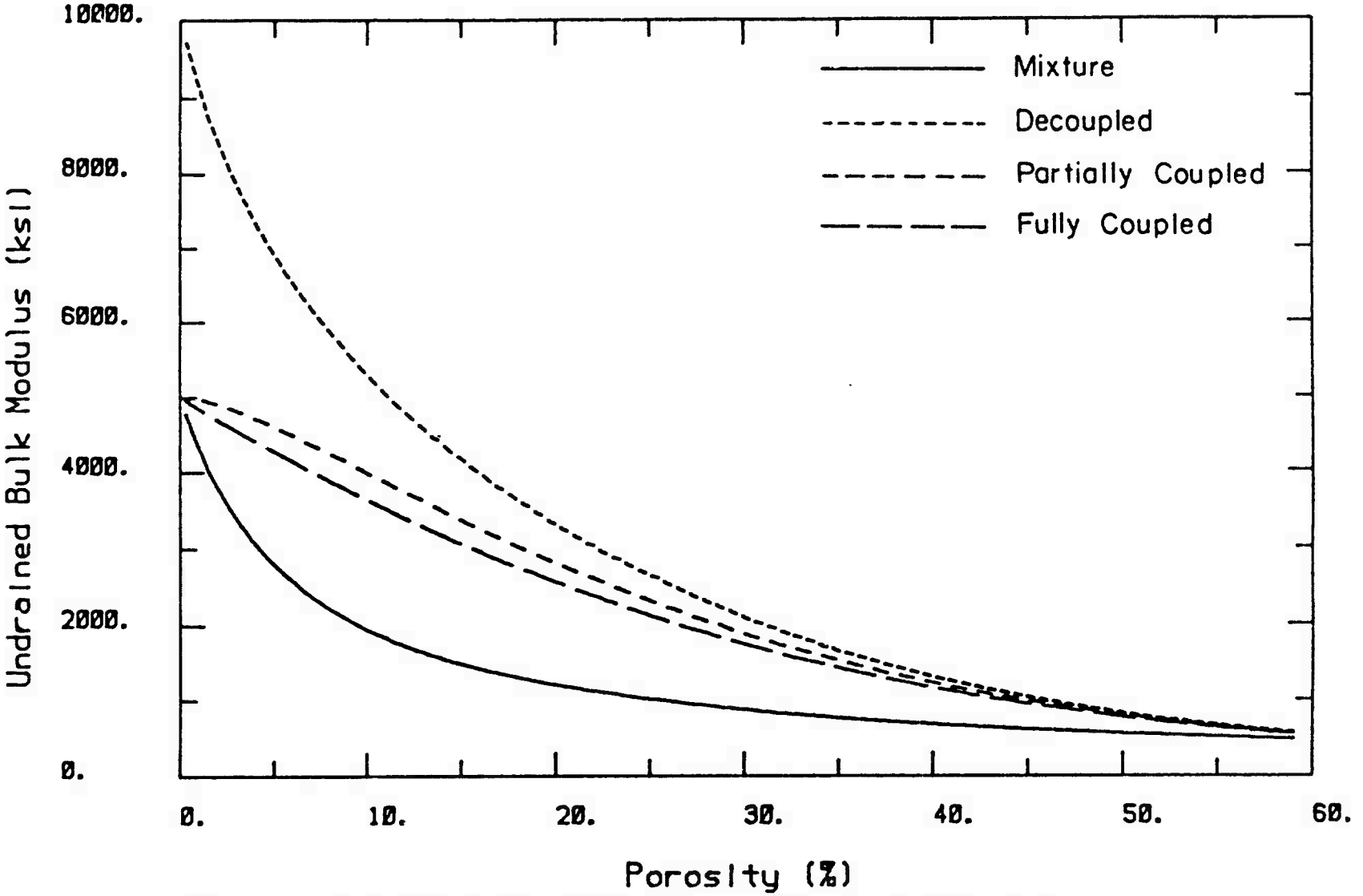

Figure 7a. Undrained bulk modulus as a function of porosity, coral.

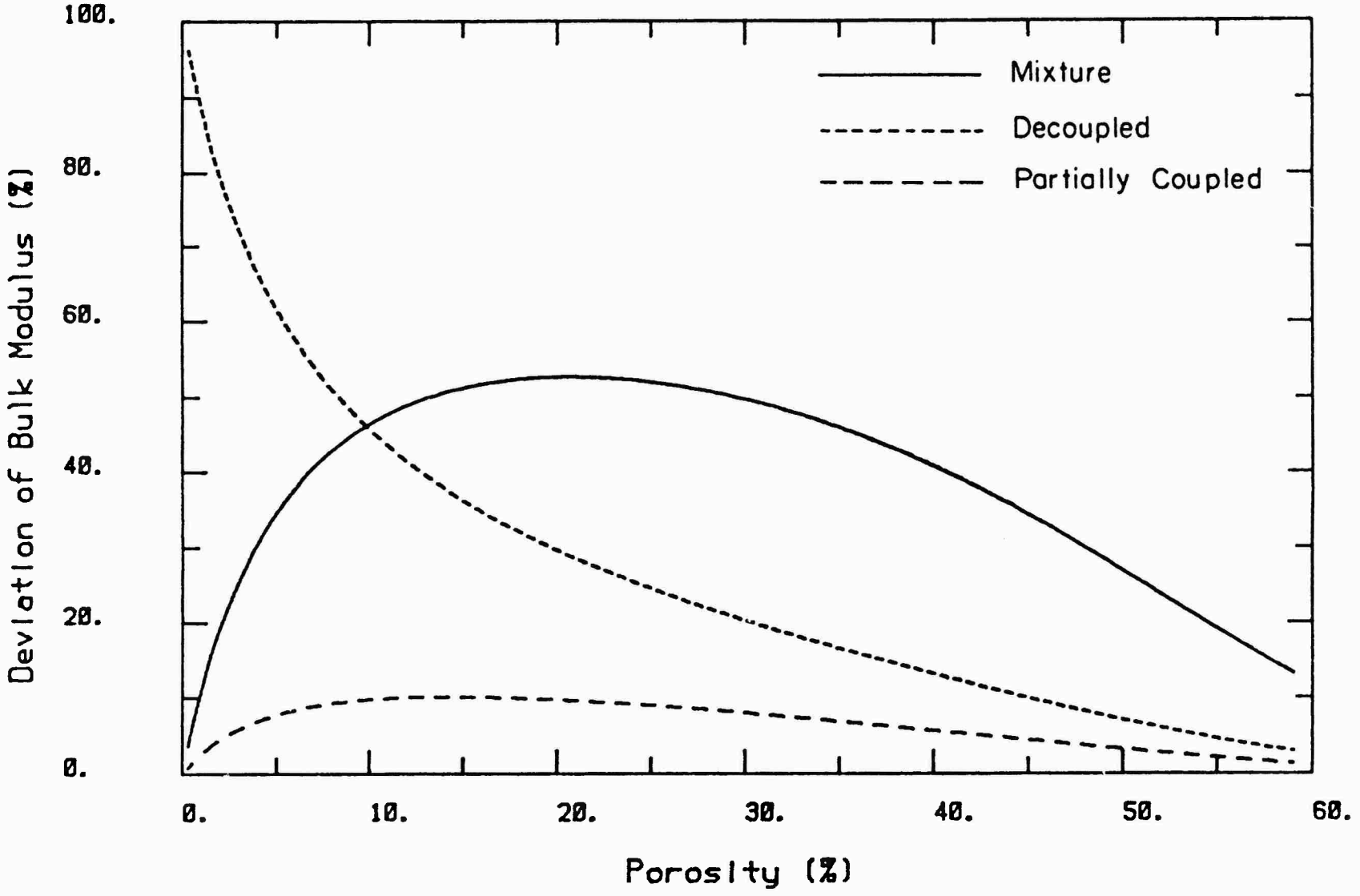

Figure 7b. Undrained bulk modulus for coral, deviation from fully coupled model.

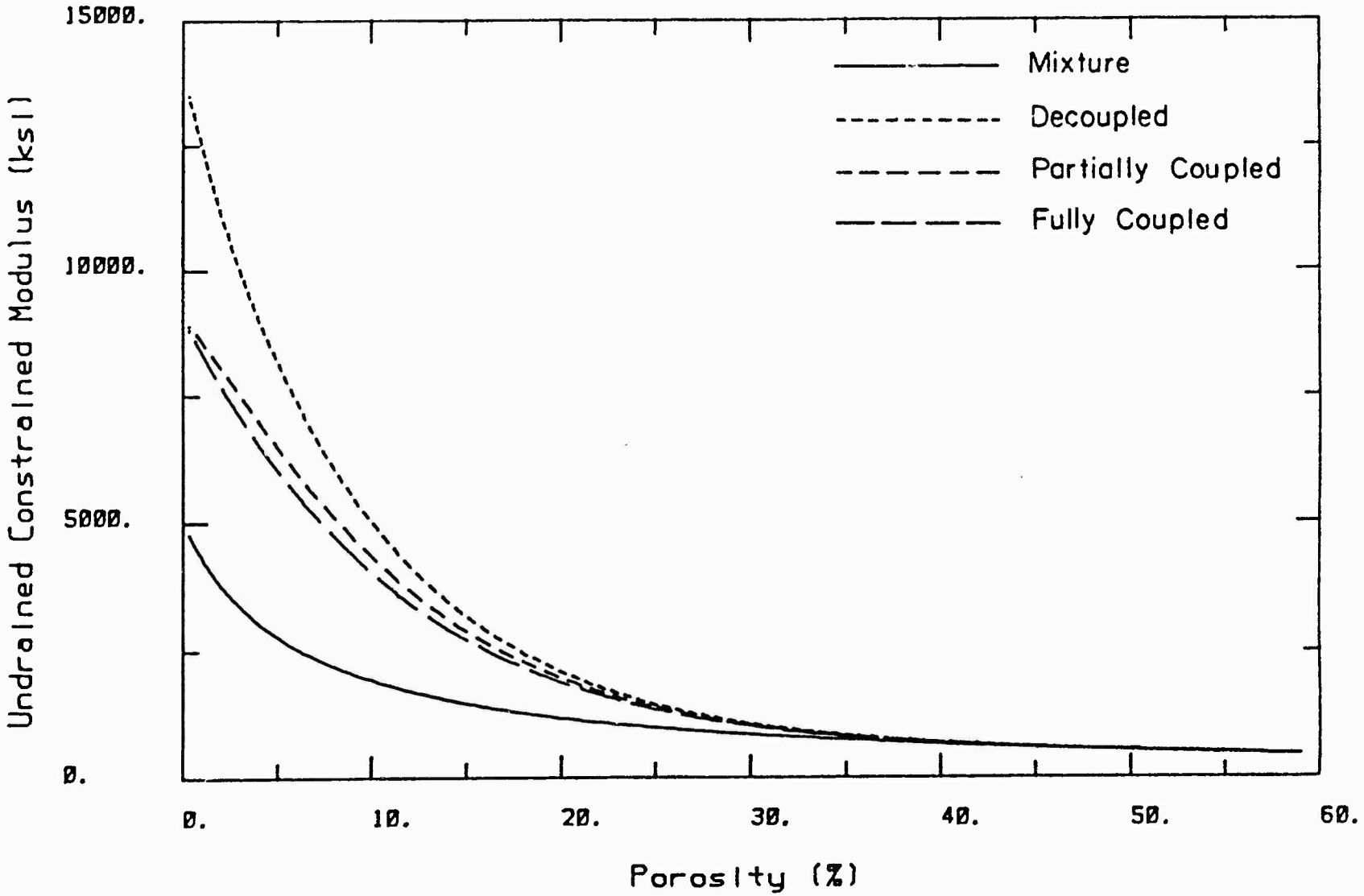

Figure 8a. Undrained constrained modulus as a function of porosity, uncemented sand.

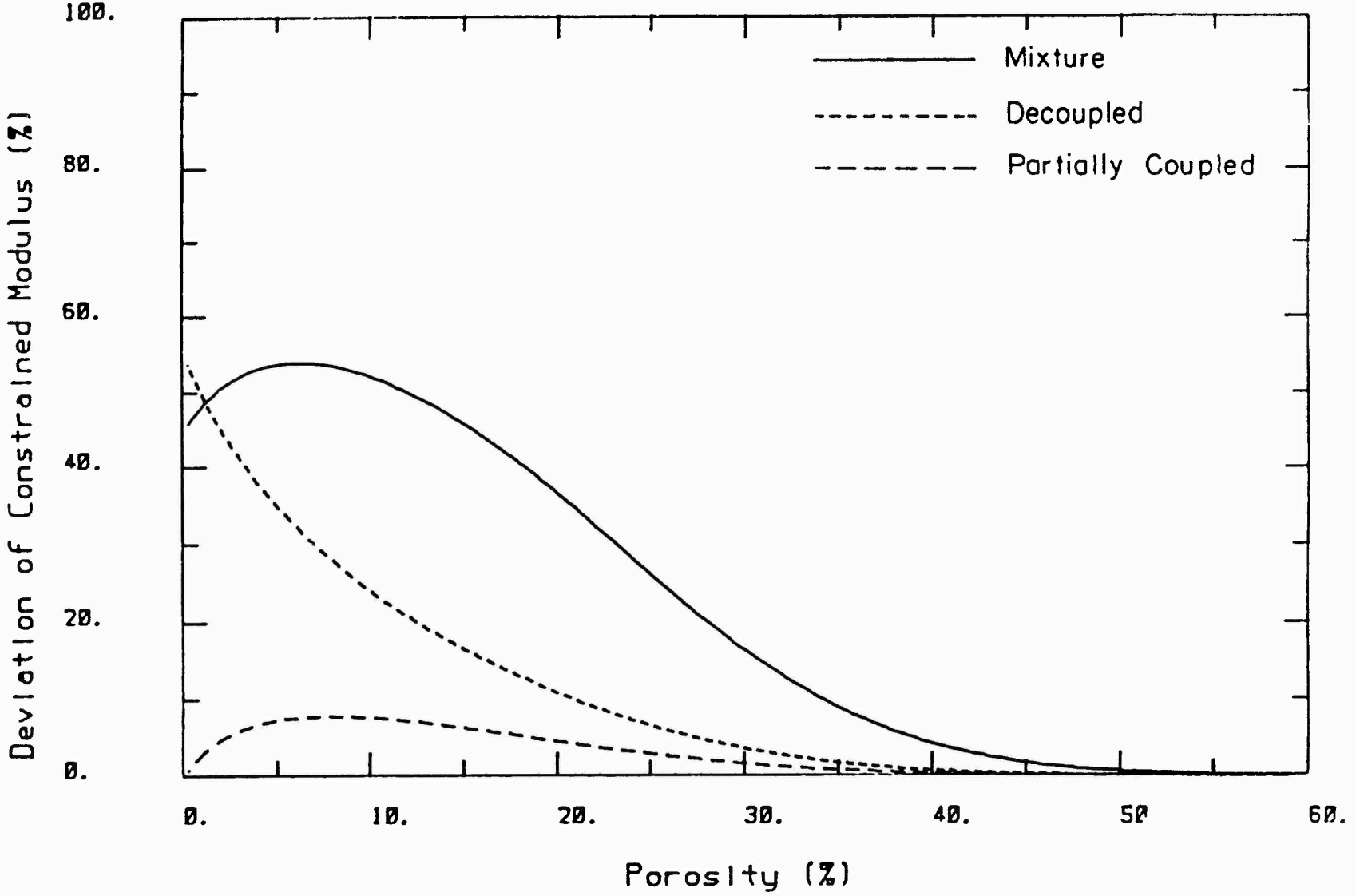

Figure 8b. Unc ined constrained modulus for uncemented sand, deviation from fully coupled model.

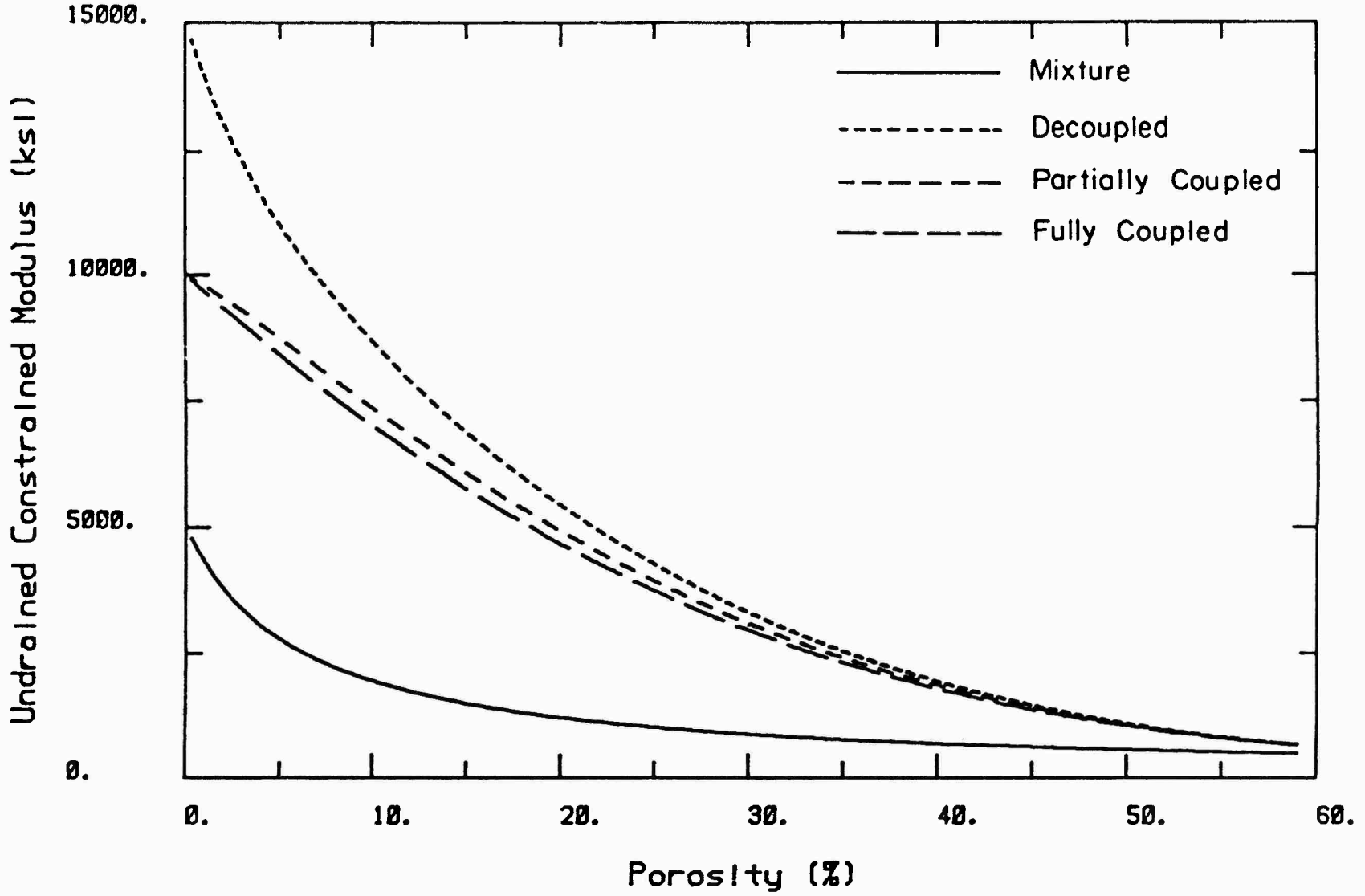

Figure 9a. Undrained constrained modulus as a function of porosity, coral.

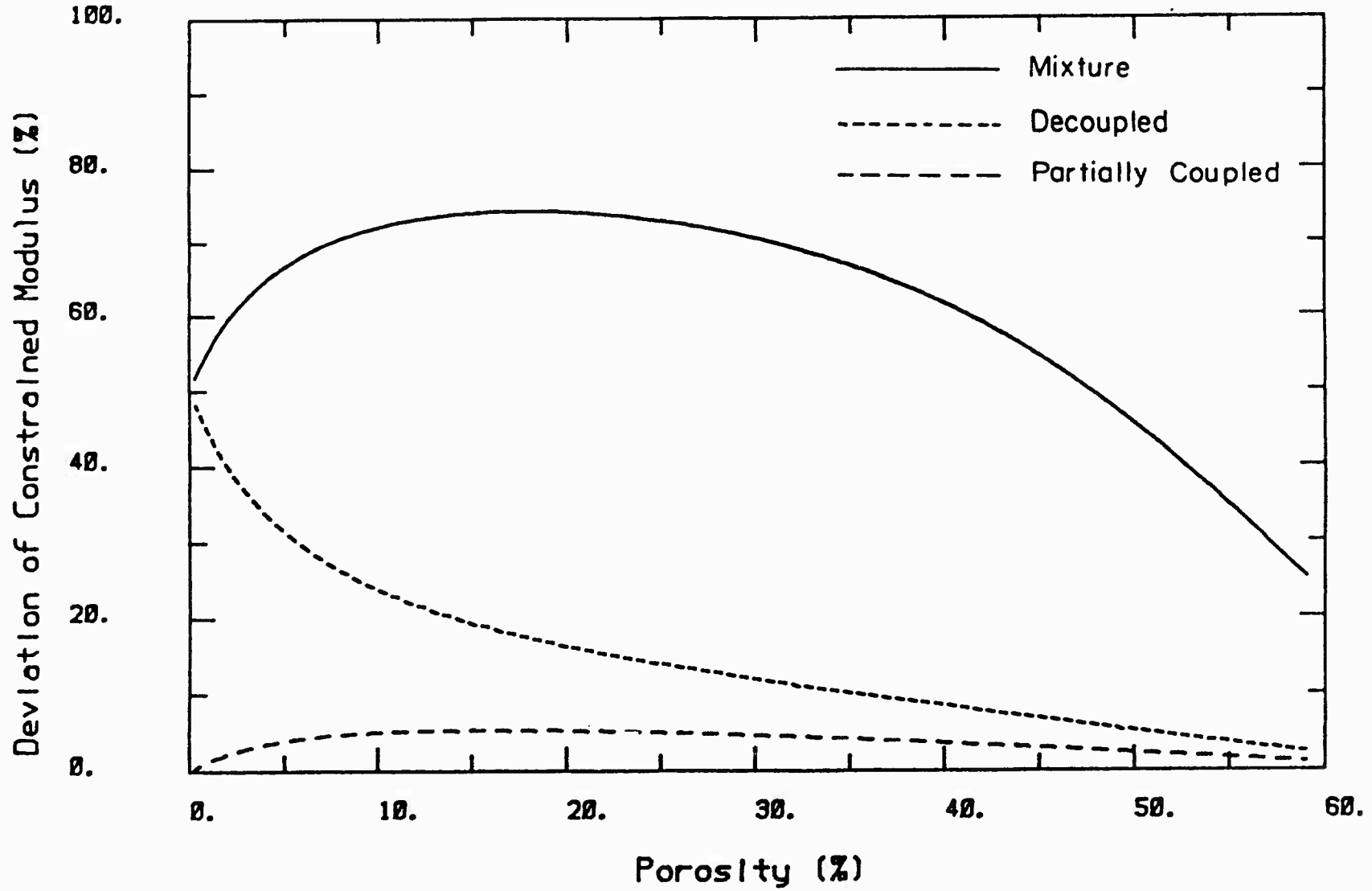

Figure 9b. Undrained constrained modulus for coral, deviation from fully coupled model.

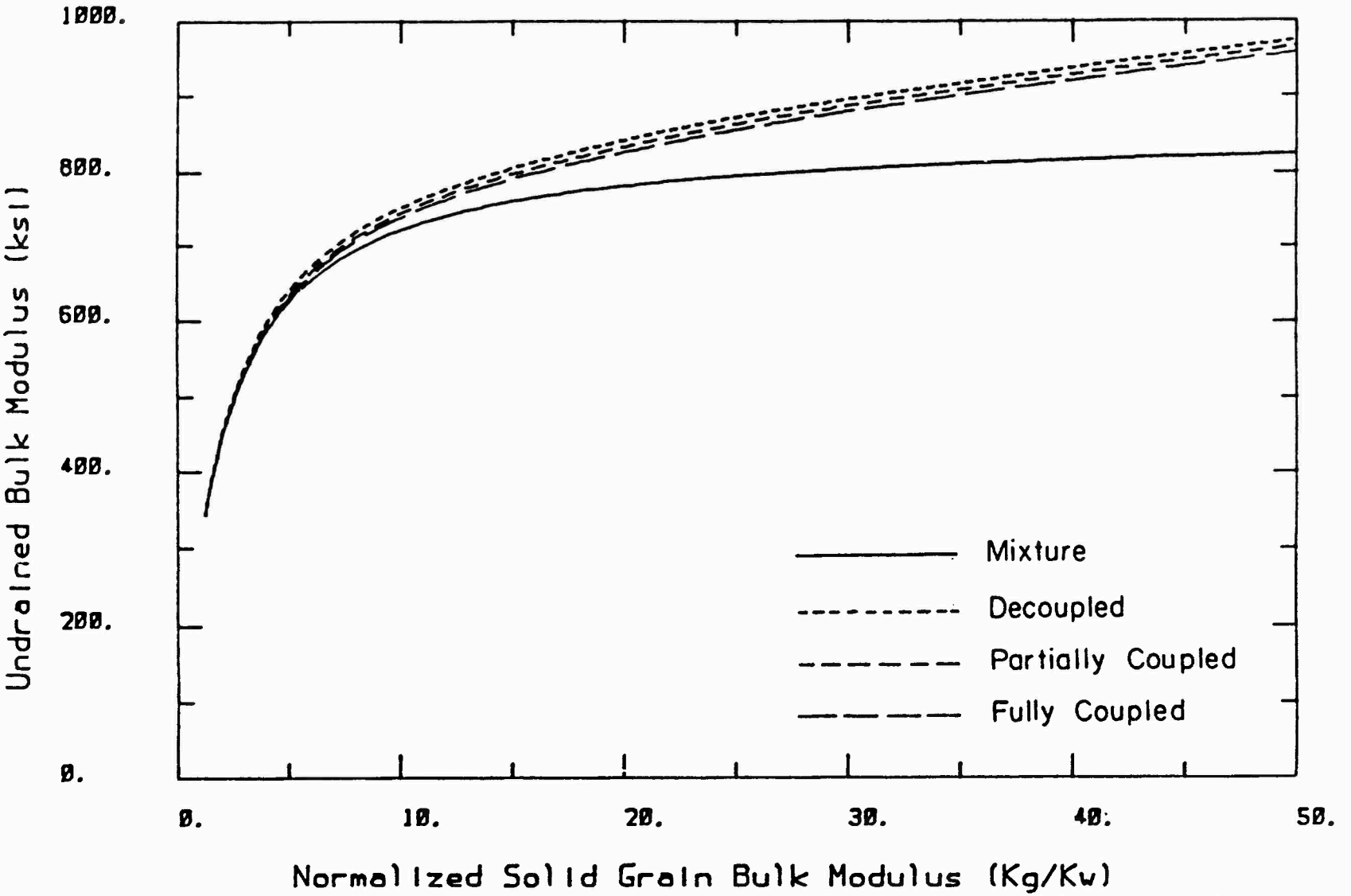

Figure 10a. Undrained bulk modulus as a function of grain bulk modulus, uncemented sand at 35% porosity.

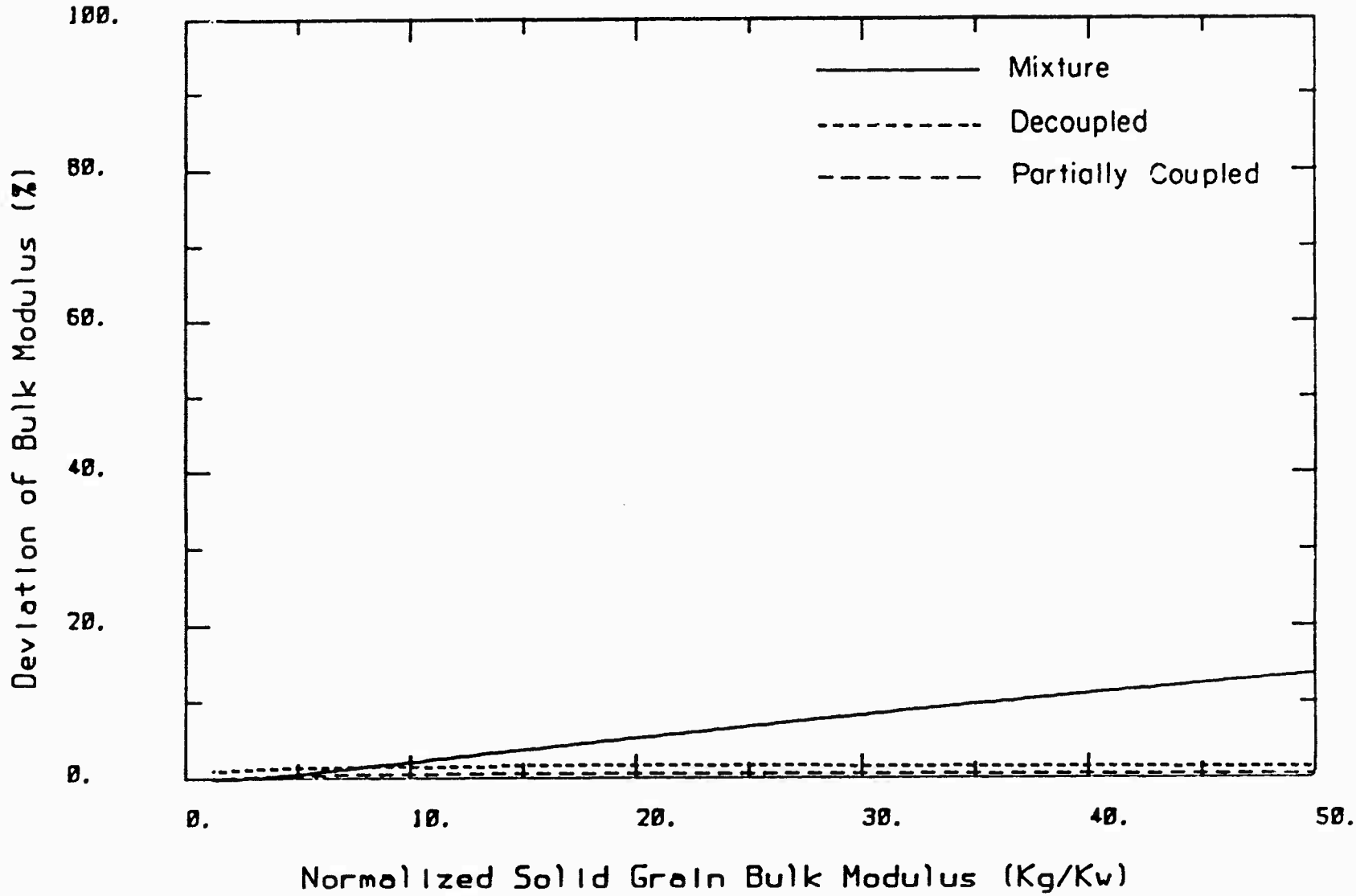

Figure 10b. Undrained bulk modulus for uncemented sand at 35% porosity, deviation from fully coupled model.

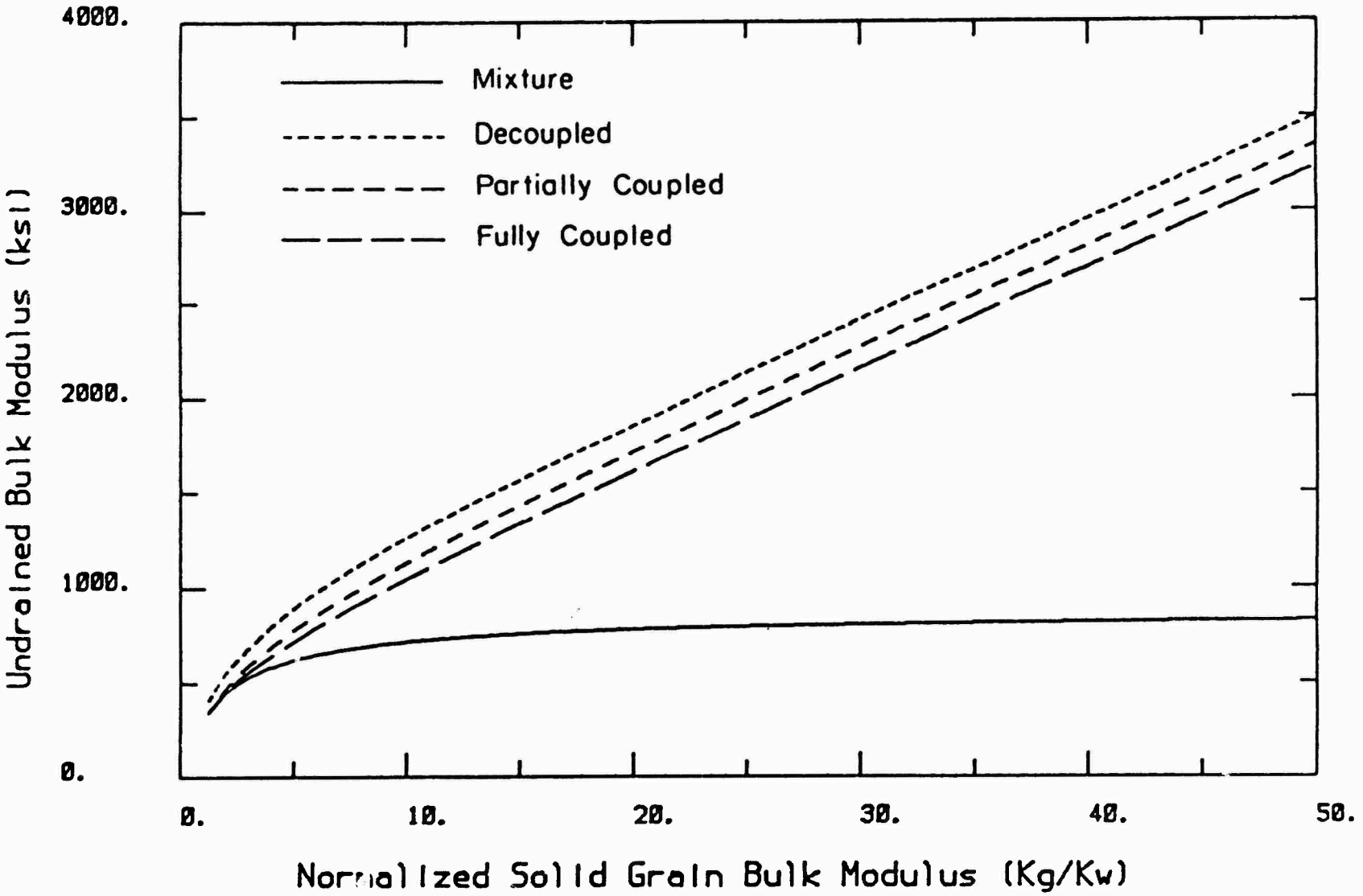

Figure 11a. Undrained bulk modulus as a function of grain bulk modulus, coral at 35% porosity.

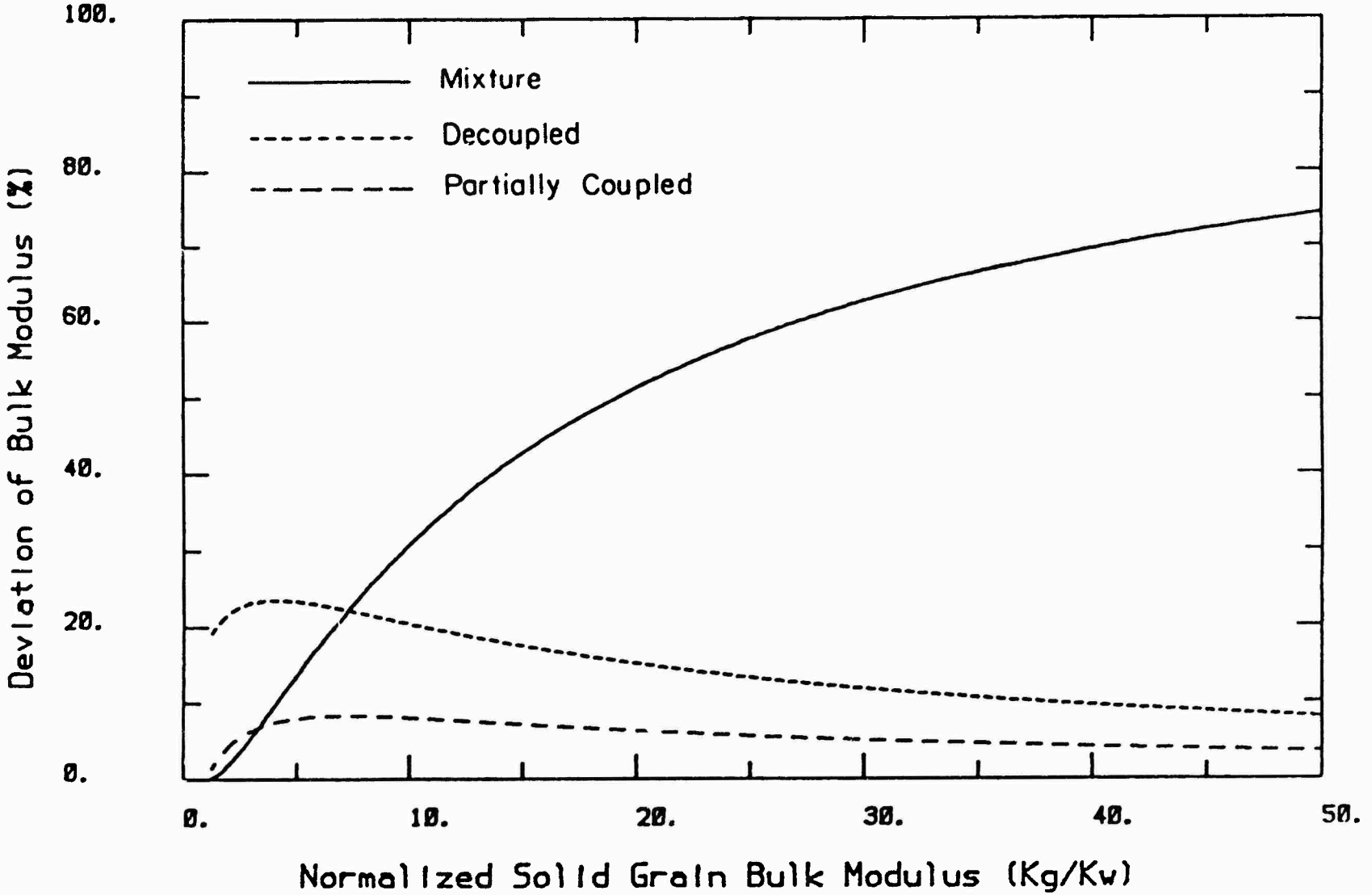

Figure 11b. Undrained bulk modulus for coral at 35% porosity, deviation from fully coupled model.

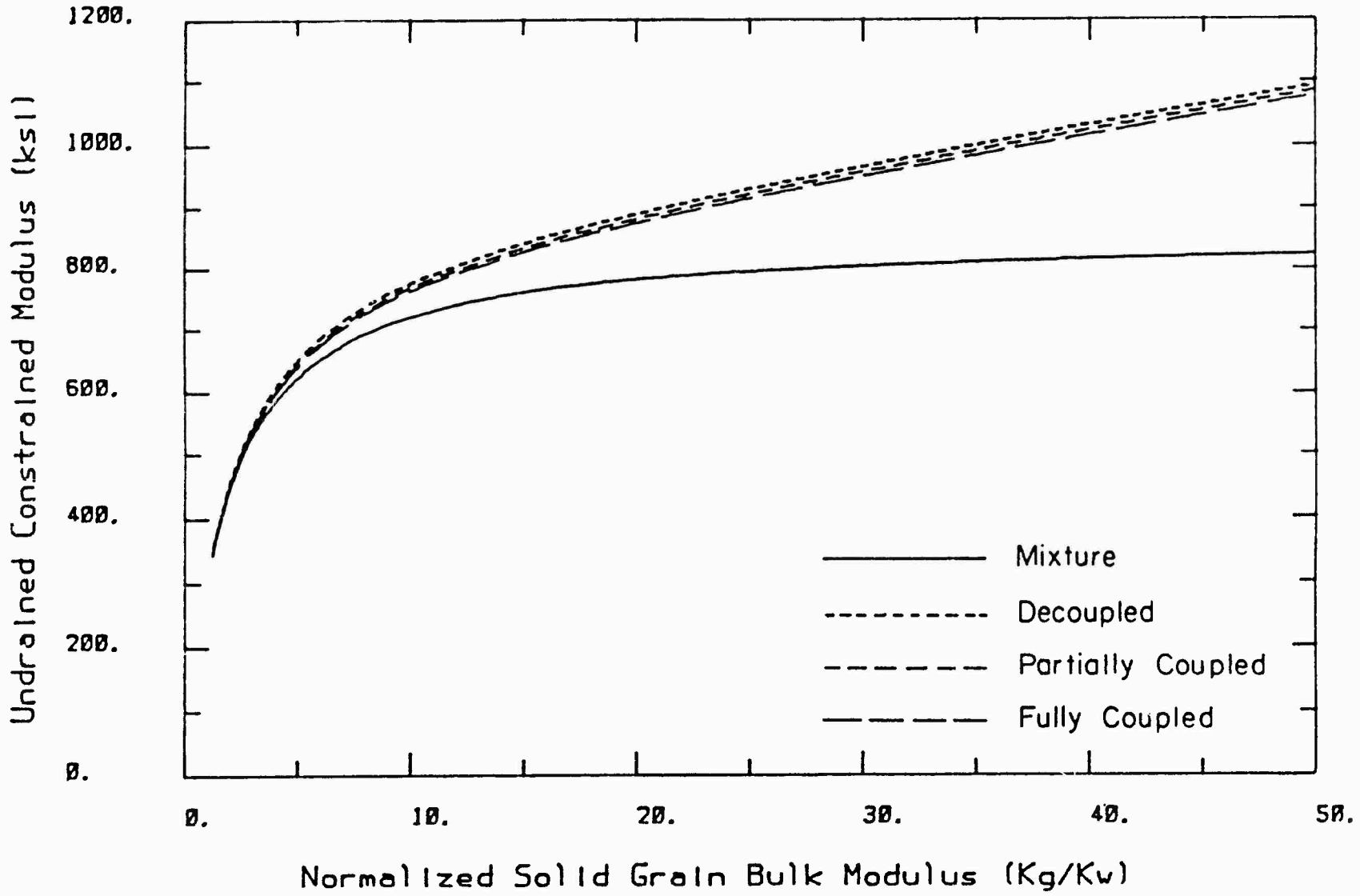

Figure 12a. Undrained constrained modulus as a function of grain bulk modulus, uncemented sand at 35% porosity.

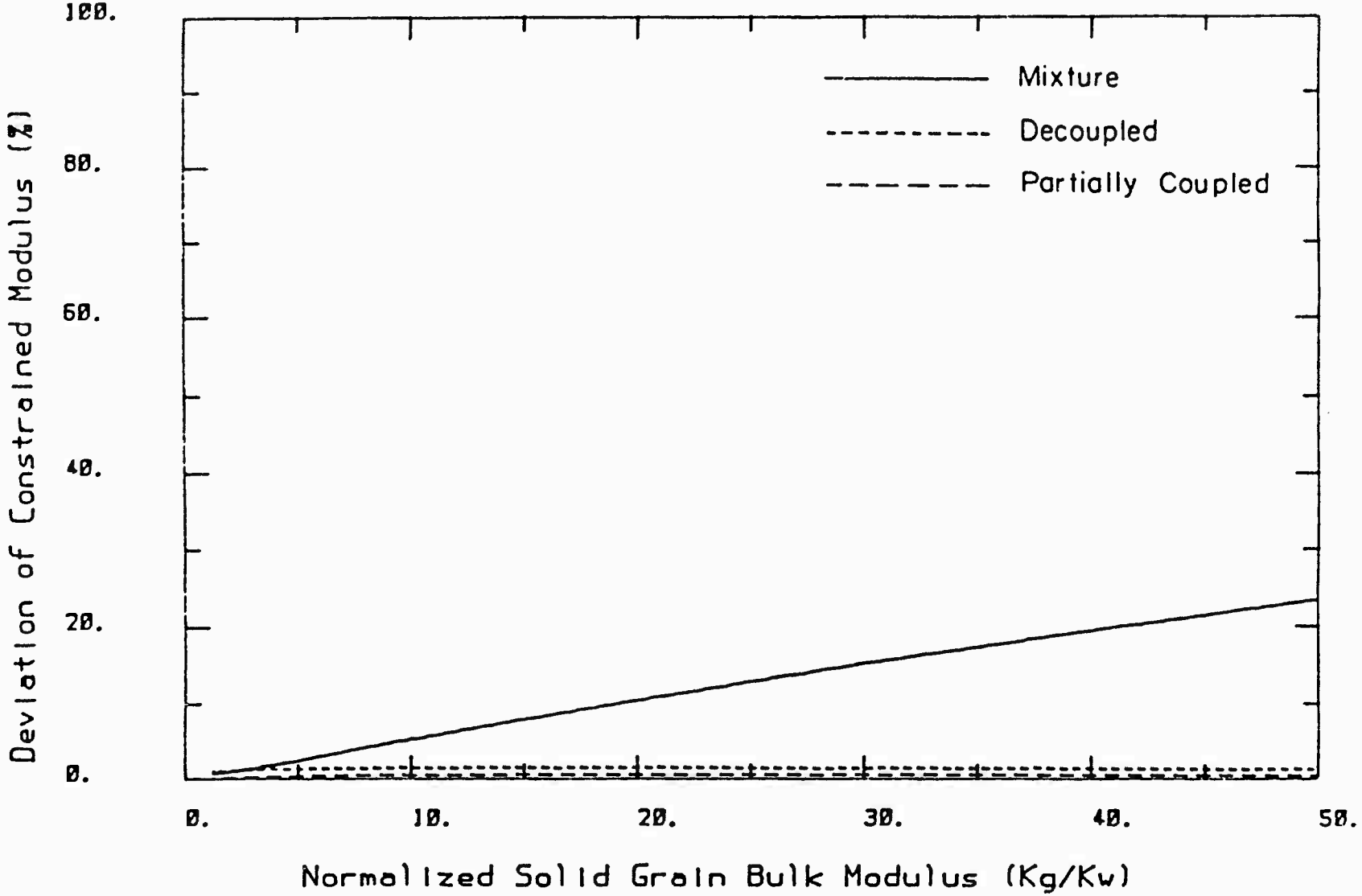

Figure 12b. ıdrained constrained modulus for uncemented sand at 35% porosity, .eviation from fully coupled model.

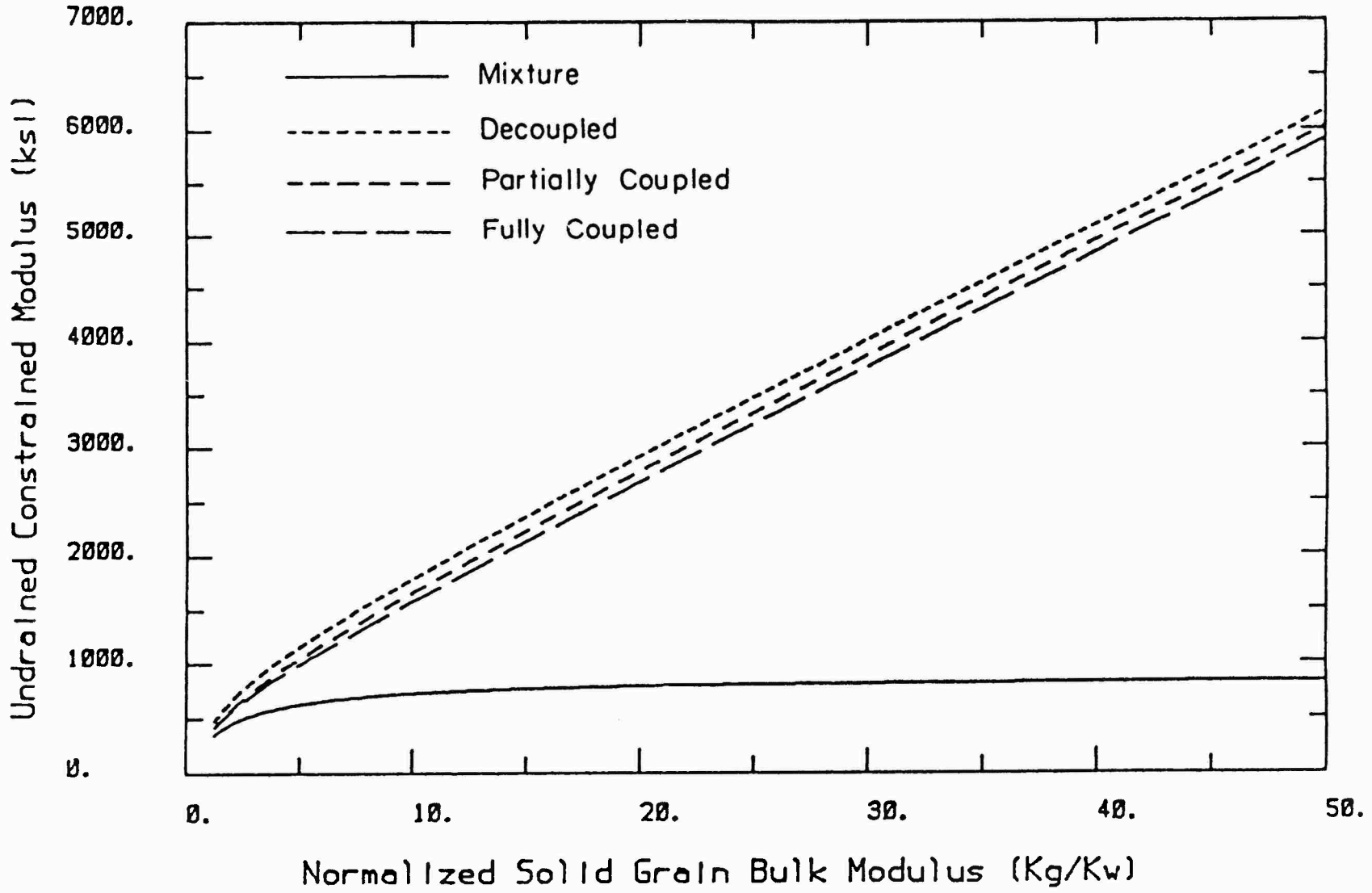

Figure 13a. Undrained constrained modulus as a function of grain bulk modulus, coral at 35% porosity.

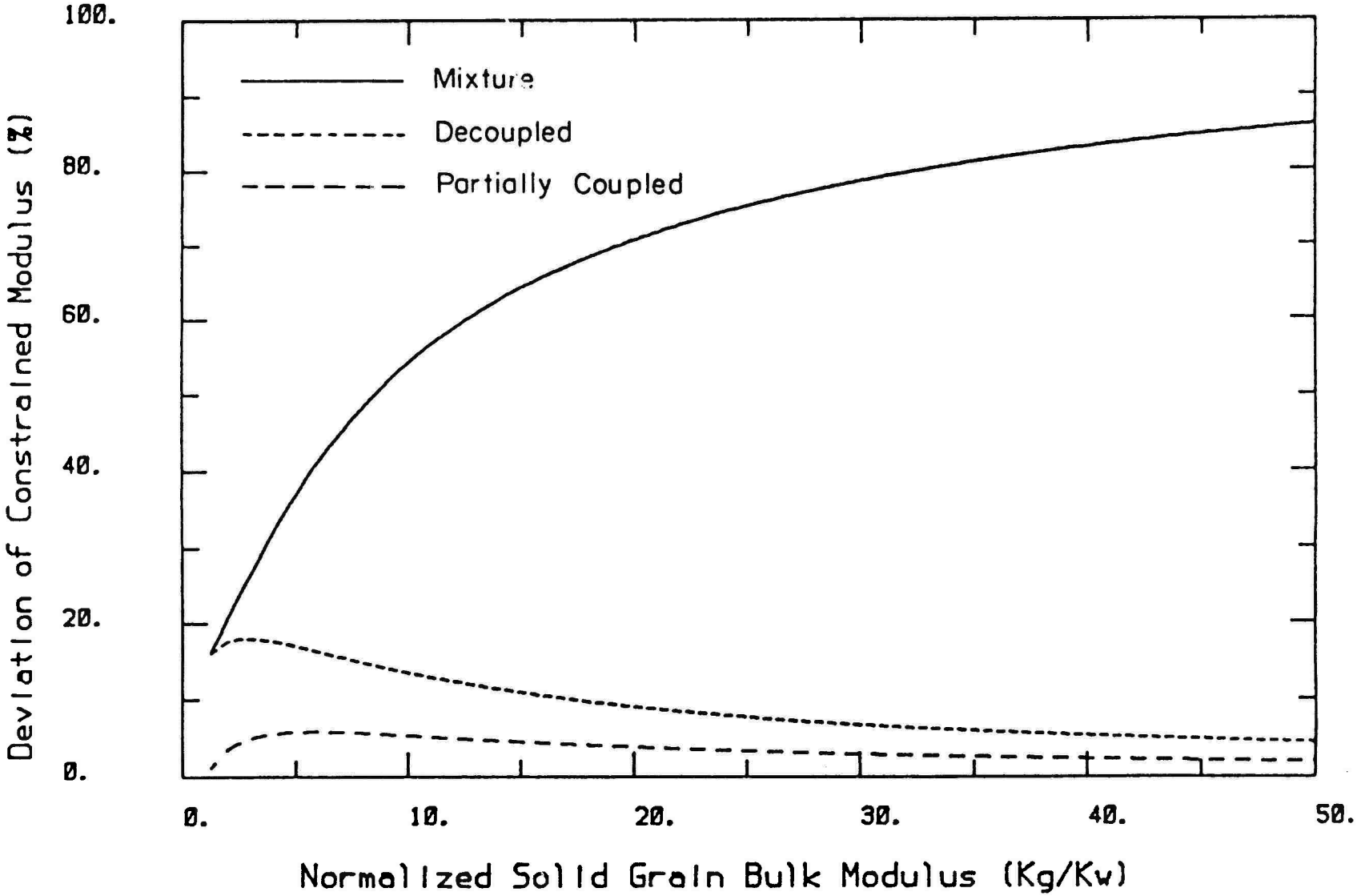

Figure 13b. Undrained constrained modulus for coral at 35% porosity, deviation from fully coupled model.

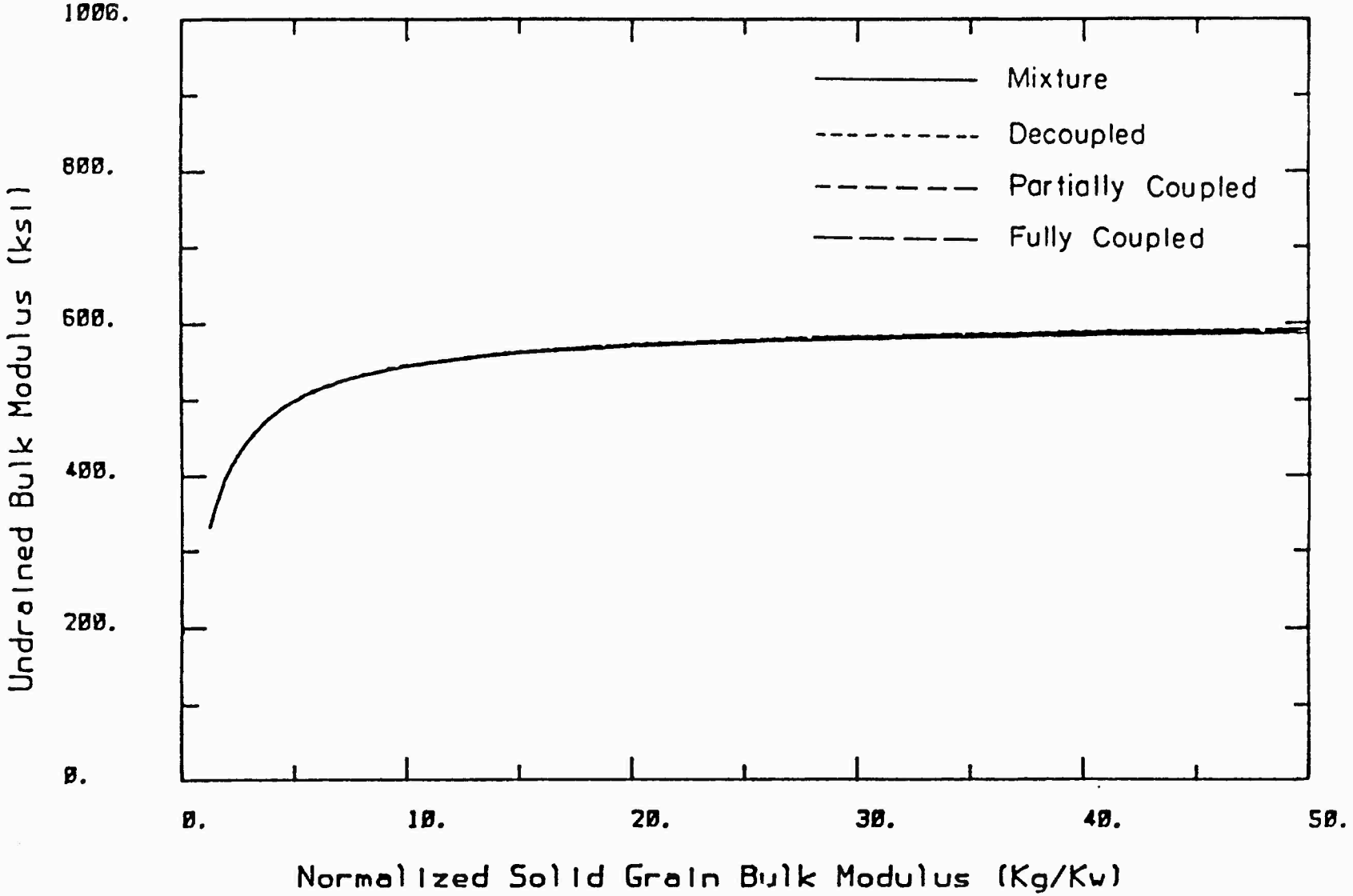

Figure 14a. Undrained bulk modulus as a function of grain bulk modulus, uncemented sand at 50% porosity.

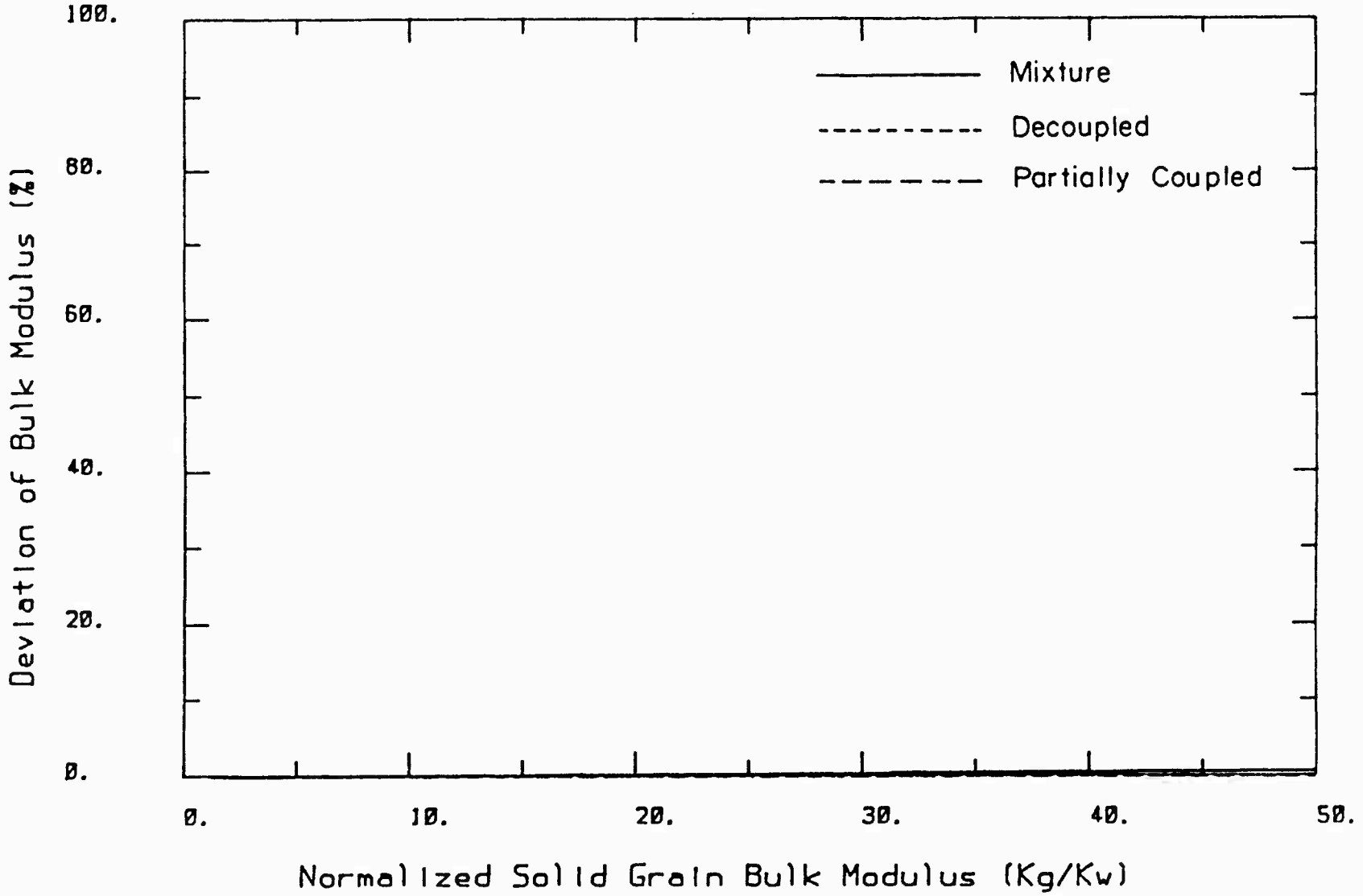

Figure 14b. Undrained bulk modulus for uncemented sand at 50% porosity, deviation from fully coupled model.

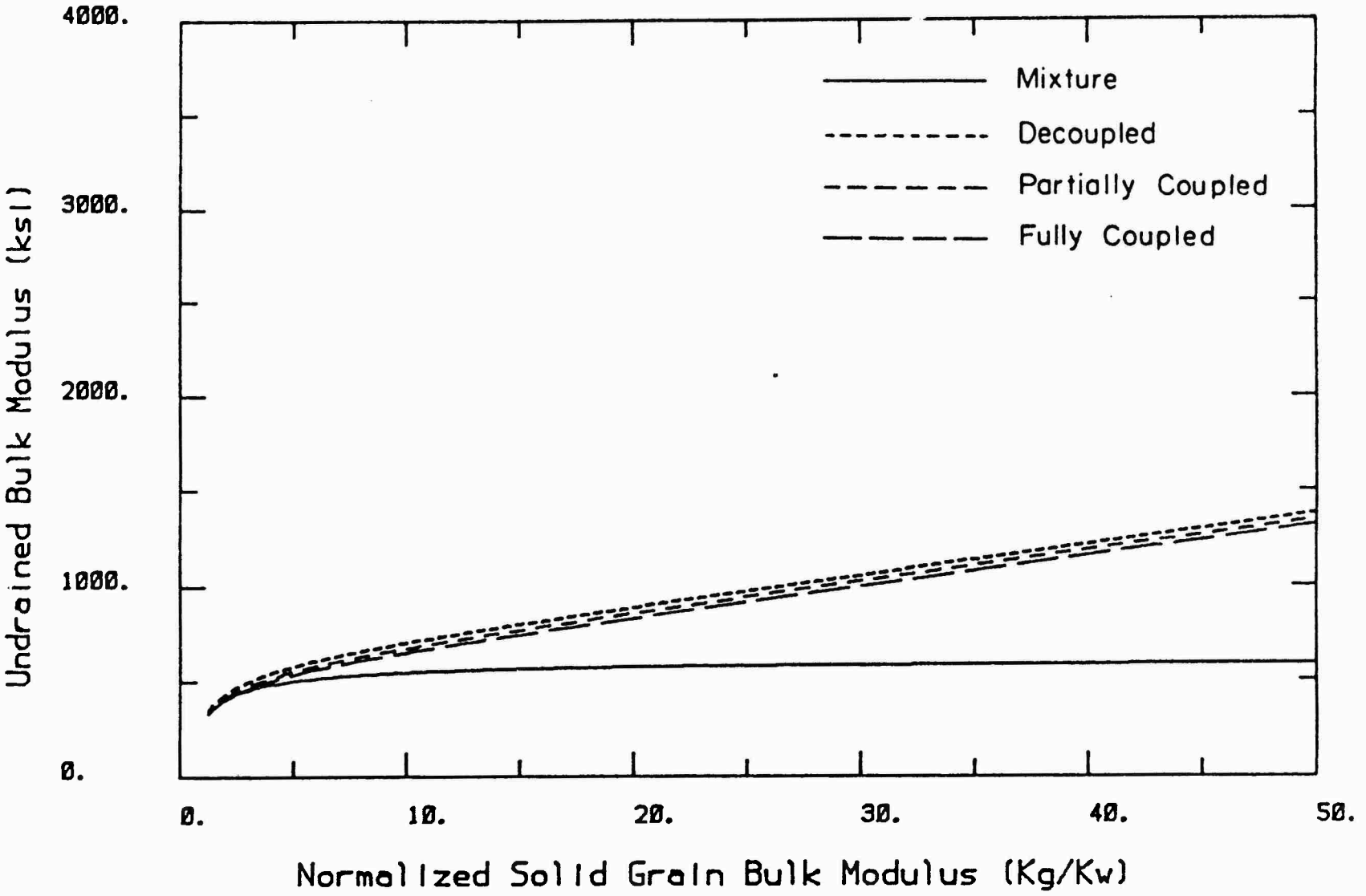

Figure 15a. Undrained bulk modulus as a function of grain bulk modulus, coral at 50% porosity.

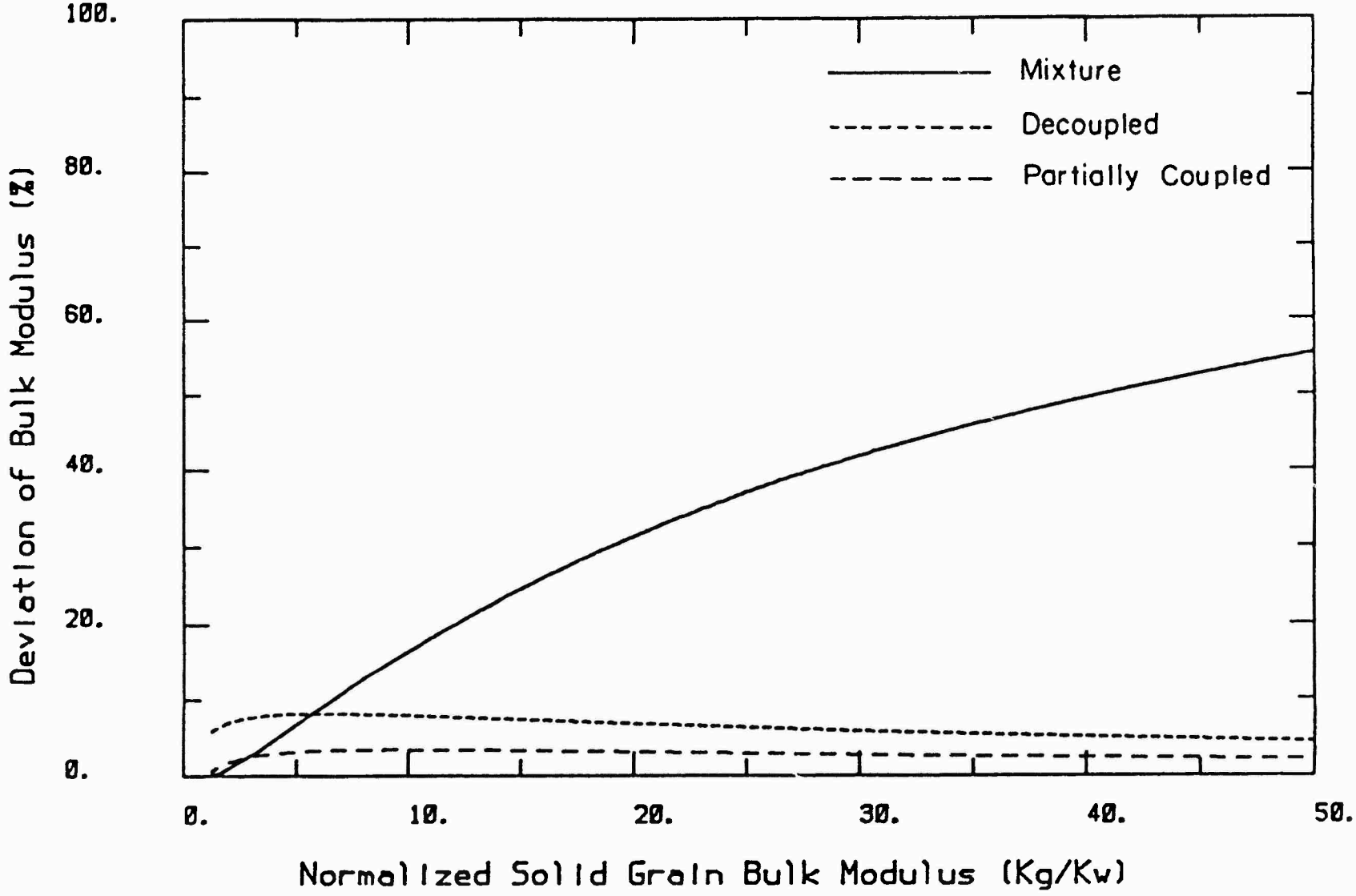

Figure 15b. Undrained bulk modulus for coral at 50% porosity, deviation from fully coupled model.

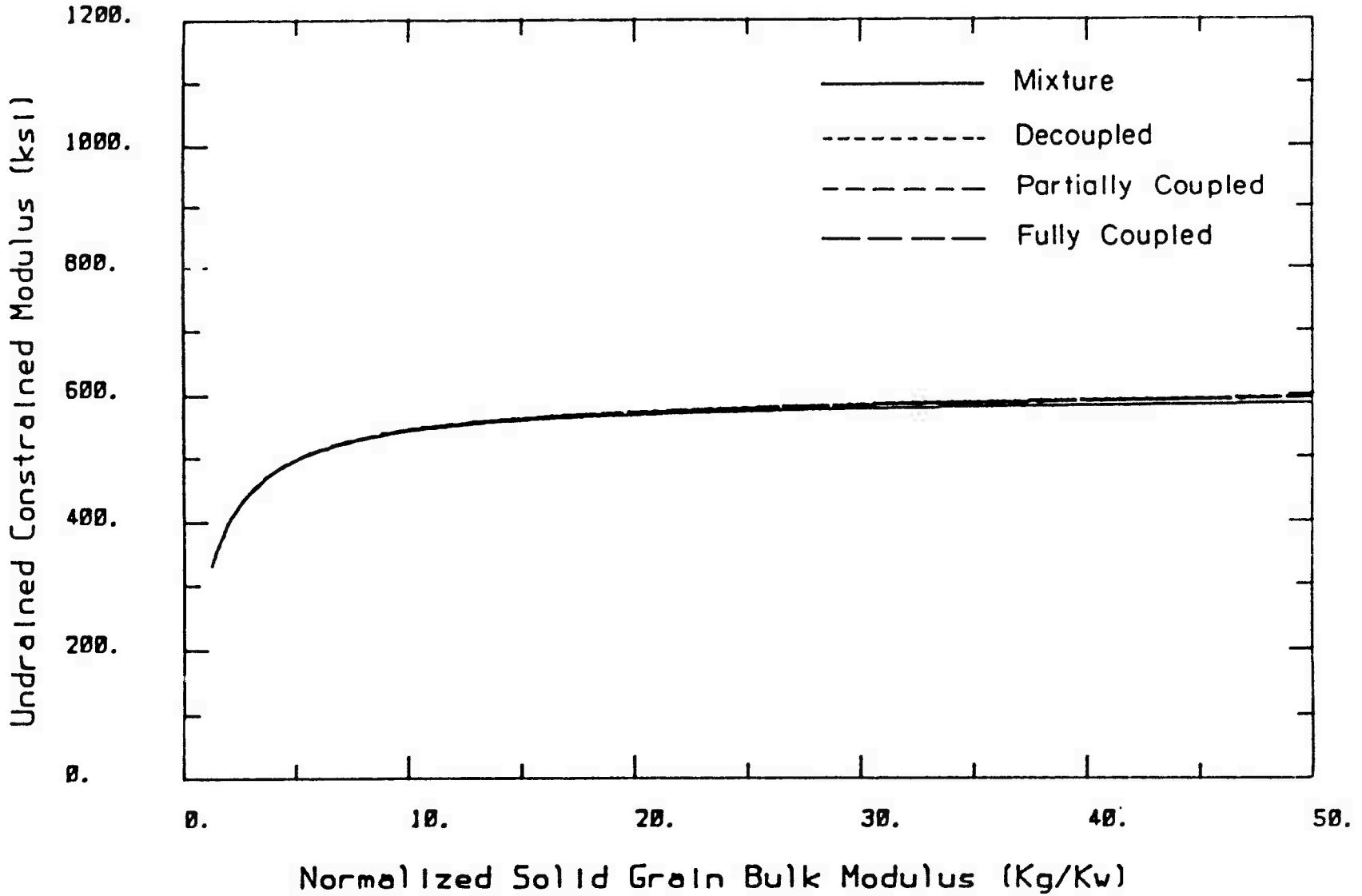

Figure 16. Undrained constrained modulus as a function of grain bulk modulus, uncemented sand at 50% porosity.

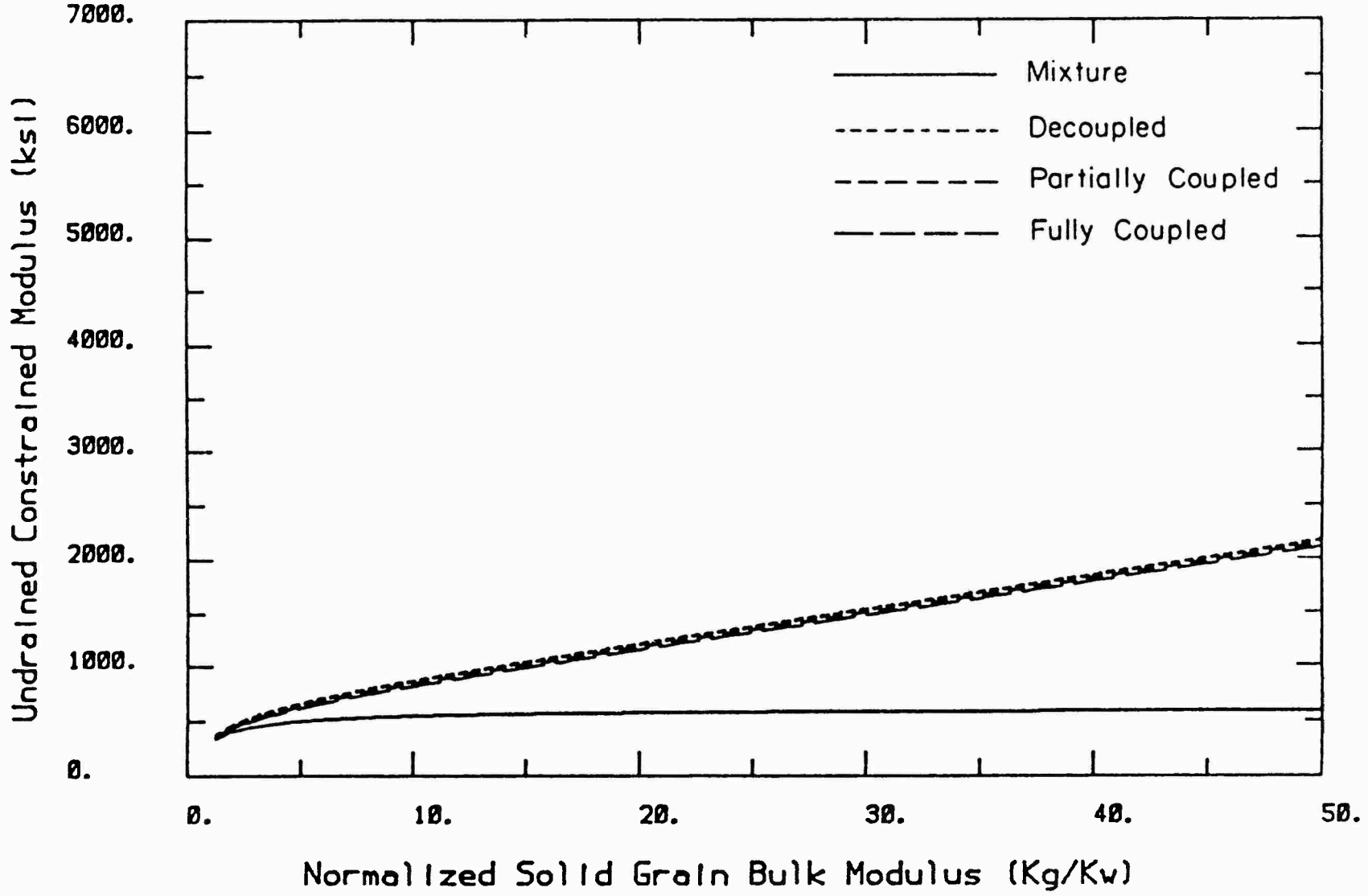

Figure 17a. Undrained constrained modulus as a function of grain bulk modulus, coral at 50% porosity.

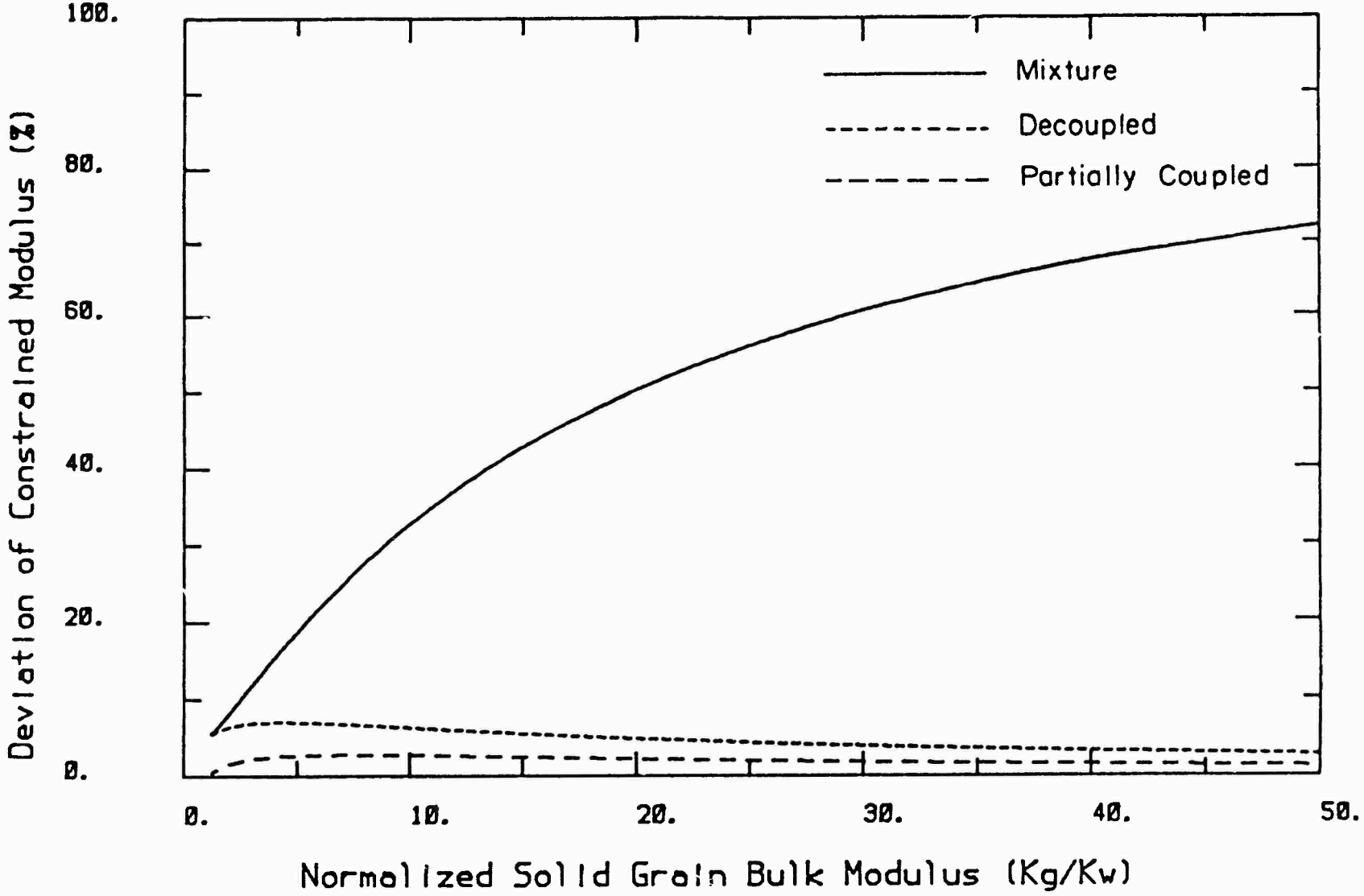

Figure 17b. Undrained constrained modulus for coral at 50% porosity, deviation from fully coupled model.

LIST OF REFERENCES

Clay, C.S., and H. Medwin, Acoustical Oceanography: Principles and Applications, John Wiley & Sons, New York, 1977.

Gassmann, F., "Uber die Elastizitat Poroser Medien," VIERTELJAHRSSCHRIFT DER NATURFORSCHENDEN GESELLSCHAFT IN ZURICH, Jahrgang 96, Heft 1, March 1951, pp. 1 - 23.

Hamilton, E.L., "Elastic Properties of Marine Sediments," J. Geophys. Res., Vol. 76, No. 2, January, 1971, pp. 579 - 604.

Merkle, D.H., and W.C. Dass, "Fundamental Properties of Soils for Complex Dynamic Loadings: Annual Technical Report No. 3," Applied Research Associates, Inc., Albuquerque, NM, December 1983.

Richart, F.E., Woods, R.D., and J.R. Hall, Jr., Vibrations of Soils and Foundations, Prentice-Hall, Inc., Englewood Cliffs, NJ, 1970.

DISTRIBUTION LIST

DEPARTMENT OF DEFENSE

DEFENSE INTELLIGENCE AGENCY
ATTN: RTS-2B
ATTN: VP-TPO

DEFENSE NUCLEAR AGENCY
2 CYS ATTN: DFSP G ULLRICH
ATTN: RAEE
ATTN: SPST
2 CYS ATTN: SPST M PELKEY
ATTN: SPST M REED
ATTN: TDTR
4 CYS ATTN: TITL

DEFENSE TECHNICAL INFORMATION CENTER
12 CYS ATTN: DD

FIELD COMMAND DEFENSE NUCLEAR AGENCY
ATTN: FCTXE
ATTN: FTCG
ATTN: FTTD
ATTN: FTTD W SUMMA

FIELD COMMAND/DNA
ATTN: FC-1

JOINT STRAT TGT PLANNING STAFF
ATTN: JK (ATTN: DNA REP)
ATTN: JKCS
ATTN: JPEP
ATTN: JPPFM
ATTN: JPST
ATTN: JPTM

DEPARTMENT OF THE ARMY

HARRY DIAMOND LABORATORIES
ATTN: SCHLD-NW-P
ATTN: SLCIS-IM-TL (81100) (TECH LIB)

U S ARMY BALLISTIC RESEARCH LAB
ATTN: SLCBR-SS-T (TECH LIB)

U S ARMY CORPS OF ENGINEERS
ATTN: DAEN-MCD-D
ATTN: DAEN-RDL

U S ARMY ENGINEER CTR & FT BELVOIR
ATTN: DT-LRC

U S ARMY ENGINEER DIV HUNTSVILLE
ATTN: HNDED-SY

U S ARMY ENGINEER DIV OHIO RIVER
ATTN: ORDAS-L (TECH LIB)

U S ARMY ENGR WATERWAYS EXPER STATION
2 CYS ATTN: J JACKSON, WESSD
ATTN: J ZELASKO, WESSD-R
ATTN: TECHNICAL LIBRARY
ATTN: WESSE (J K INGRAM)

U S ARMY MATERIAL COMMAND
ATTN: DRXAM-TL (TECH LIB)

U S ARMY MATERIAL TECHNOLOGY LABORATORY
ATTN: TECHNICAL LIBRARY

U S ARMY MISSILE COMMAND
ATTN: DOCUMENTS, AMSMI-RD-CS-R

U S ARMY NUCLEAR & CHEMICAL AGENCY
ATTN: LIBRARY

U S ARMY STRATEGIC DEFENSE COMMAND
ATTN: DASD-H-L
ATTN: ICRDAHB-X

DEPARTMENT OF THE NAVY

NAVAL FACILITIES ENGINEERING COMMAND
ATTN: CODE 04B

NAVAL POSTGRADUATE SCHOOL
ATTN: CODE 1424 LIBRARY

NAVAL RESEARCH LABORATORY
ATTN: CODE 2627 (TECH LIB)

NAVAL SURFACE WEAPONS CENTER
ATTN: TECH LIBRARY & INFO SVCS BR

NAVAL WEAPONS EVALUATION FACILITY
ATTN: CLASSIFIED LIBRARY

OFC OF THE DEPUTY CHIEF OF NAVAL OPS
ATTN: OP 03EG
ATTN: OP 981

OFFICE OF NAVAL RESEARCH
ATTN: CODE 1132SM

SPACE & NAVAL WARFARE SYSTEMS CMD
ATTN: PME 117-21

STRATEGIC SYSTEMS PROGRAM OFFICE (PM-1)
ATTN: NSP-L63 (TECH LIB)

DEPARTMENT OF THE AIR FORCE

AFIS/INT
ATTN: INT

AIR FORCE GEOPHYSICS LABORATORY
ATTN: LWH/H OSSING

AIR FORCE INSTITUTE OF TECHNOLOGY/EN
ATTN: LIBRARY/AFIT/LDEE

AIR FORCE SYSTEMS COMMAND
ATTN: DLW

AIR FORCE WEAPONS LABORATORY, NTAAB
ATTN: NTE M PLAMONDON
ATTN: NTED J THOMAS
ATTN: NTED R HENNY
ATTN: NTES
ATTN: NTES-G
ATTN: SUL

AIR UNIVERSITY LIBRARY
ATTN: AUL-LSE

BALLISTIC MISSILE OFFICE/DAA
ATTN: ENS
ATTN: ENSN

DEPUTY CHIEF OF STAFF
LOGISTICS & ENGINEERING
ATTN: LEEE

DEPUTY CHIEF OF STAFF/AF-RDQM
ATTN: AF/RDQI

ROME AIR DEVELOPMENT CENTER, AFSC
ATTN: TECHNICAL LIBRARY (DOVL)

STRATEGIC AIR COMMAND/INA
ATTN: INA

STRATEGIC AIR COMMAND/NRI-STINFO
ATTN: NRI/STINFO

STRATEGIC AIR COMMAND/XPQ
ATTN: XPQ

DEPARTMENT OF ENERGY

DEPARTMENT OF ENERGY
ATTN: R JONES

DEPARTMENT OF ENERGY
ATTN: DOC CON PUBLIC AFFAIRS TECH

LAWRENCE LIVERMORE NATIONAL LAB
ATTN: A RATCLIFFE
ATTN: D BURTON
ATTN: D CLARKE
ATTN: L-221 D GLENN
ATTN: L-53 TECH INFO DEPT. LIBRARY
ATTN: L-84 H KRUGER
ATTN: W CROWLEY

LOS ALAMOS NATIONAL LABORATORY
ATTN: C F KELLER
ATTN: D218 MS M HENDERSON
ATTN: F601 T DOWLER
ATTN: J LILLEY
ATTN: REPORT LIBRARY
ATTN: J SARRACINO

OAK RIDGE NATIONAL LABORATORY
ATTN: CENTRAL RSCH LIBRARY
ATTN: CIVIL DEF RES PROJ

SANDIA NATIONAL LABORATORIES
ATTN: EDUCATION AND TECH LIB DIV

SANDIA NATIONAL LABORATORIES
ATTN: DIV 7111 J S PHILLIPS
ATTN: J M MCGLAUN 6444
ATTN: ORG 7111 L R HILL
ATTN: ORG 7112 A CHABAI
ATTN: T K BERGSTRESSER 1531
ATTN: TECH LIB 3141 (RPTS RECEIVING CLRK)
ATTN: W R DAVEY 1533

OTHER GOVERNMENT

CENTRAL INTELLIGENCE AGENCY
ATTN: OSWR/NED

DEPARTMENT OF THE INTERIOR
ATTN: TECH LIB

DEPARTMENT OF THE INTERIOR
ATTN: D RODDY

DEPARTMENT OF DEFENSE CONTRACTORS

AEROSPACE CORP
ATTN: LIBRARY ACQUISITION

APPLIED RESEARCH ASSOCIATES, INC
ATTN: N HIGGINS

APPLIED RESEARCH ASSOCIATES, INC
2 CYS ATTN: J KWANG
2 CYS ATTN: S BLOUIN

APPLIED RESEARCH ASSOCIATES, INC
ATTN: D PIEPENBURG

APPLIED RESEARCH ASSOCIATES, INC
ATTN: R FRANK

BDM CORP
ATTN: CORPORATE LIB

BDM CORP
ATTN: F LEECH

BOEING CO
ATTN: R SCHMIDT
ATTN: H WICKLEIN

CALIFORNIA INSTITUTE OF TECHNOLOGY
ATTN: T AHRENS

CALIFORNIA RESEARCH & TECHNOLOGY, INC
ATTN: K KREYENHAGEN
ATTN: LIBRARY
ATTN: M ROSENBLATT
ATTN: S SCHUSTER

CALIFORNIA RESEARCH & TECHNOLOGY, INC
ATTN: F SAUER

DENVER COLORADO SEMINARY UNIVERSITY OF
ATTN: J WISOTSKI

IIT RESEARCH INSTITUTE
ATTN: A BUTI
ATTN: DOCUMENTS LIBRARY
ATTN: M JOHNSON

KAMAN SCIENCES CORP
ATTN: L MENTE
ATTN: LIBRARY

KAMAN SCIENCES CORP
ATTN: LIBRARY/B. KINSLOW

KAMAN TEMPO
ATTN: DASIAC

KAMAN TEMPO
ATTN: DASIAC

LOCKHEED MISSILES & SPACE CO, INC
ATTN: J BONIN

LOCKHEED MISSILES & SPACE CO, INC
ATTN: J WEISNER

MAXWELL LABORATORIES, INC
ATTN: J MURPHY

MCDONNELL DOUGLAS CORP
ATTN: R HALPRIN

MITRE CORPORATION
ATTN: J SULLIVAN

PACIFIC-SIERRA RESEARCH CORP
ATTN: H BRODE, CHAIRMAN SAGE
ATTN: L SCHLESSINGER

PACIFICA TECHNOLOGY
ATTN: R ALLEN

PATEL ENTERPRISES, INC
ATTN: M PATEL

PHYSICS INTERNATIONAL CO
ATTN: H W WAMPLER

R & D ASSOCIATES
ATTN: C K B LEE
ATTN: C MCDONALD
ATTN: D OBERSTE-LEHN
ATTN: D SIMONS
ATTN: J LEWIS
ATTN: J RADLER
ATTN: TECHNICAL INFORMATION CENTER

R & D ASSOCIATES
ATTN: G GANONG

RAND CORP
ATTN: P DAVIS

RAND CORP
ATTN: B BENNETT

S-CUBED
ATTN: B PYATT
ATTN: C DISMUKES
ATTN: D GRINE
ATTN: LIBRARY
ATTN: R LAFRENZ
ATTN: T RINEY

S-CUBED
ATTN: B L RISTVET

SCIENCE & ENGRG ASSOCIATES, INC
ATTN: J STOCKTON

SCIENCE APPLICATIONS INTL CORP
ATTN: H WILSON
ATTN: M MCKAY
ATTN: R SCHLAUG
ATTN: TECHNICAL LIBRARY
ATTN: W SCOTT
ATTN: W WOOLSON

SCIENCE APPLICATIONS INTL CORP
ATTN: D MAXWELL

SCIENCE APPLICATIONS INTL CORP
ATTN: J COCKAYNE
ATTN: W LAYSON

SOUTHWEST RESEARCH INSTITUTE
ATTN: A WENZEL

SRI INTERNATIONAL
ATTN: D KEOUGH

TELEDYNE BROWN ENGINEERING
ATTN: D ORMOND
ATTN: F LEOPARD

TERRA TEK, INC
ATTN: S GREEN

THE BDM CORPORATION
ATTN: J MERRITT
ATTN: LIBRARY

TRW SPACE & DEFENSE
2 CYS ATTN: N LIPNER
ATTN: P BHUTA
ATTN: TECH INFO CTR, DOC ACQ

WASHINGTON, UNIVERSITY OF
ATTN: J KATZ

WEIDLINGER ASSOC
ATTN: J ISENBERG

WEIDLINGER ASSOC., CONSULTING ENGRG
ATTN: T DEEVY

WEIDLINGER ASSOC, CONSULTING ENGRG
ATTN: I SANDLER
ATTN: M BARON